

Future Prospects for MeV Polarimetry

Mark McConnell

University of New Hampshire &
Southwest Research Institute



The Value of Polarimetry

- Polarization yields information about asymmetry or anisotropy inherent in the source.
- Such asymmetry may be within the source itself, or in the medium between source and observer, or both.
- It is often a good way of obtaining otherwise inaccessible information about the internal structure (geometry) of the source region.
- Energy dependence can sometimes be used to infer the emission mechanism.

At MeV energies, we are concerned only with linear polarization.

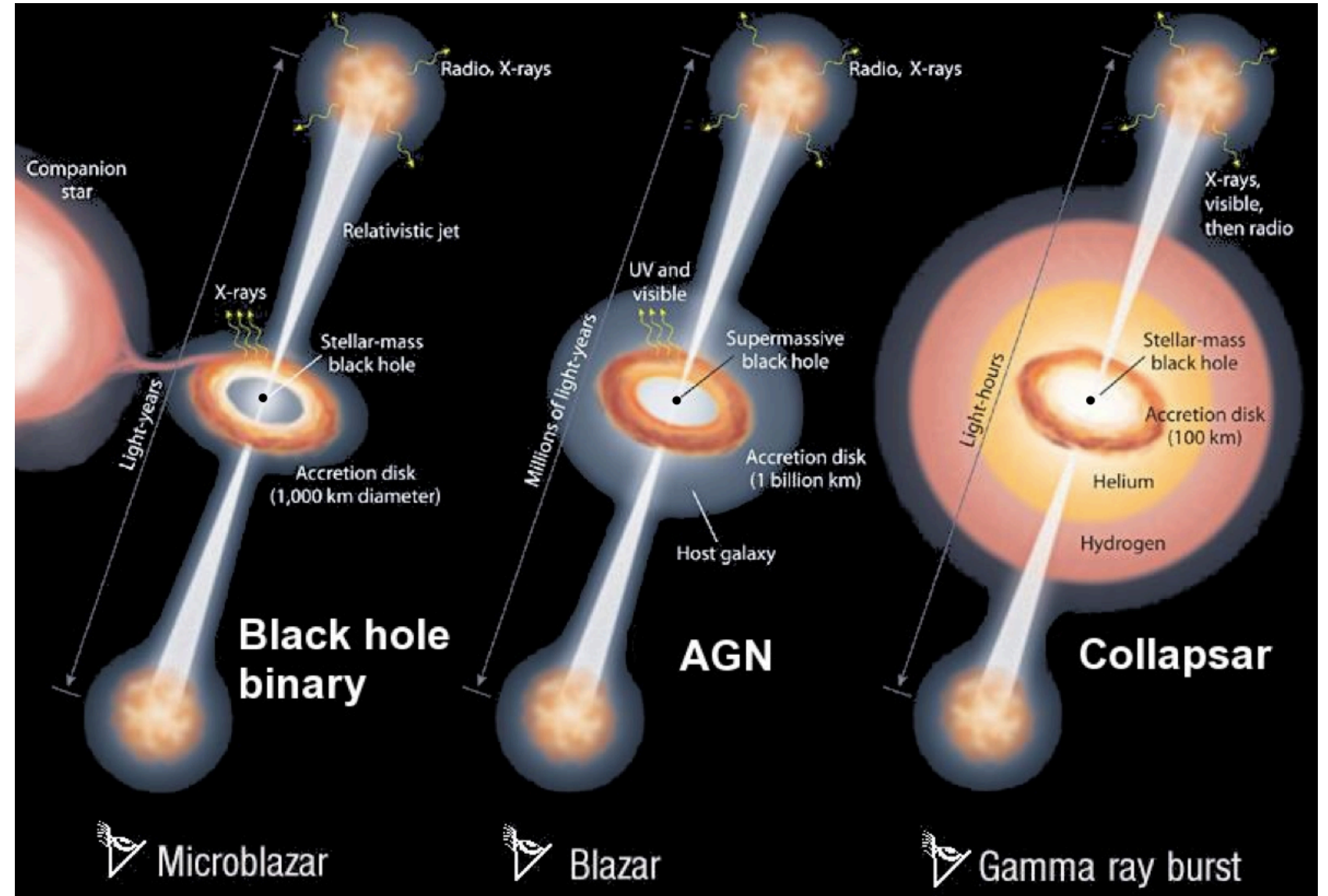
Sources of Interest

Transient sources include:

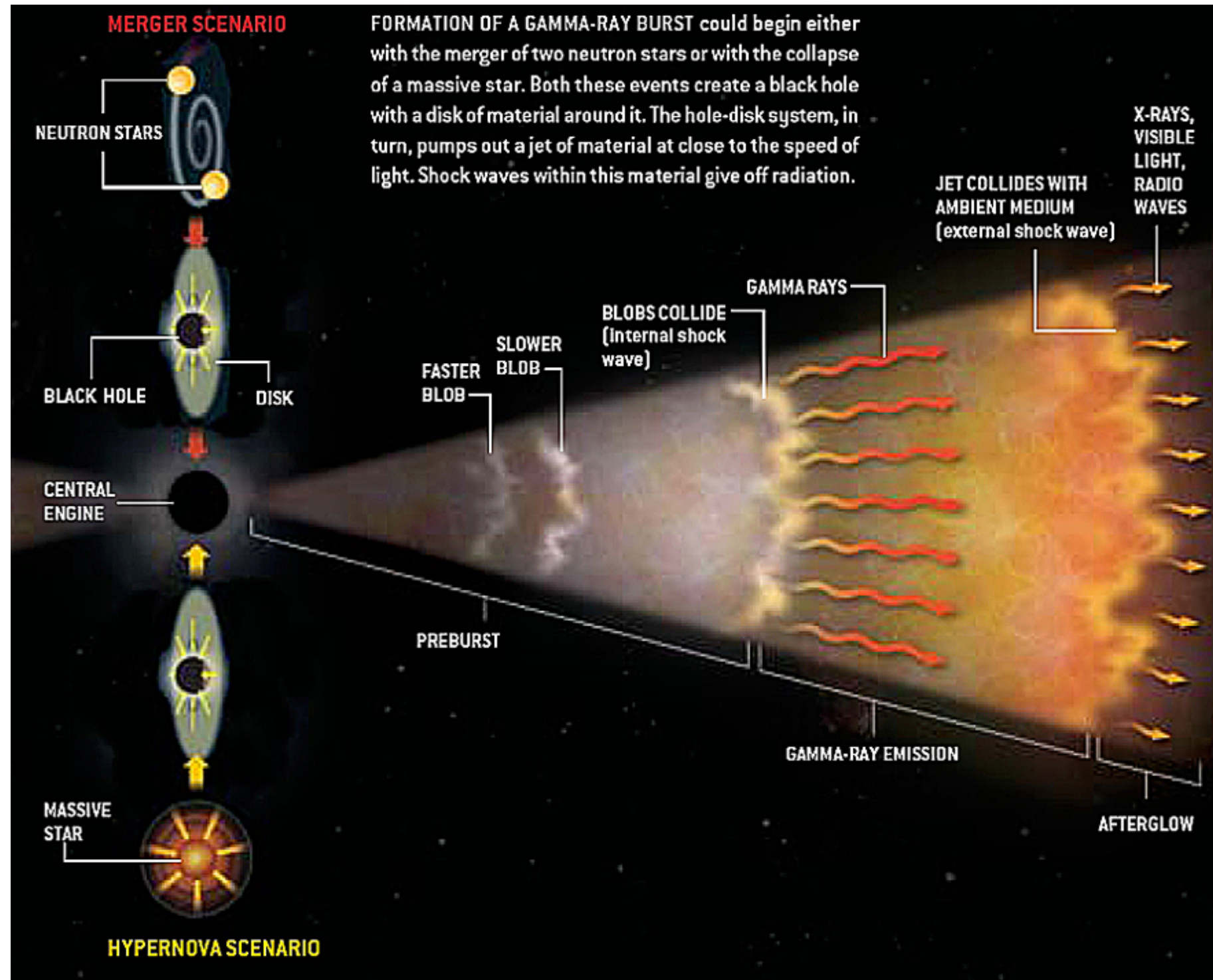
- *Gamma-Ray Bursts (GRBs)*
- *Solar Flares*

Steady (or quasi-steady) sources include:

- *Pulsars*
- *Stellar-Mass Black Holes*
- *Blazars (AGN)*

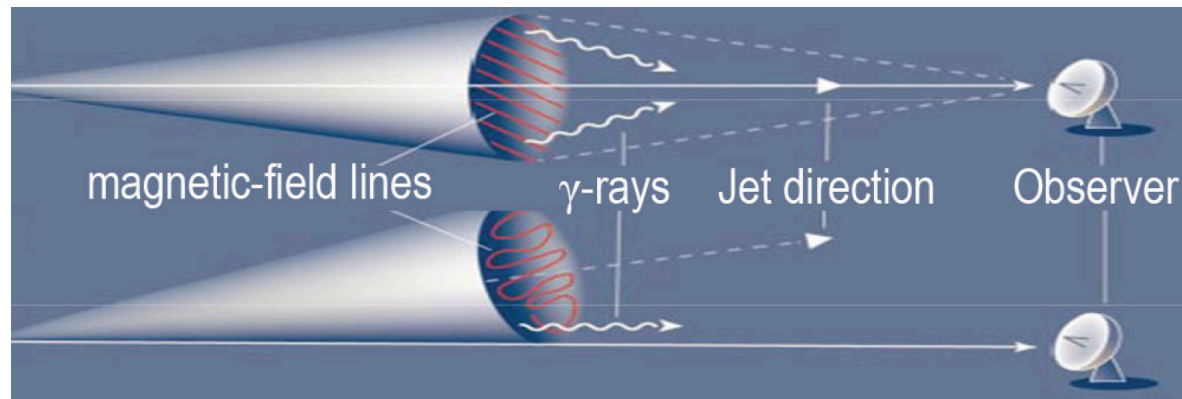


Gamma-Ray Bursts



Regardless of the progenitor, we can learn about the physical properties of the ultra-relativistic jets, including the energy dissipation sites, and the radiation mechanisms.

Objectives for GRB Polarimetry



	Intrinsic Model	Geometric Models	
Objectives	Synchrotron Ordered	Compton Drag	Synchrotron Random
1. Magnetic Field	Ordered	Random	Random
2. Jet Composition	Poynting Flux	Matter	Matter
3. Jet Energy Dissipation Mechanism	Reconnection	Internal Shocks	Internal Shocks
4. Prompt Emission Mechanism	Synchrotron	Inverse Compton	Synchrotron

Magnetic Field structure (random vs ordered)

- low polarization \Rightarrow randomly oriented B-fields
- high polarization \Rightarrow ordered B-fields

Energy dissipation (internal shocks vs reconnection)

- low polarization \Rightarrow internal shocks
- high polarization \Rightarrow reconnection

Jet Composition (matter vs Poynting flux)

- low polarization \Rightarrow matter
- high polarization \Rightarrow Poynting flux

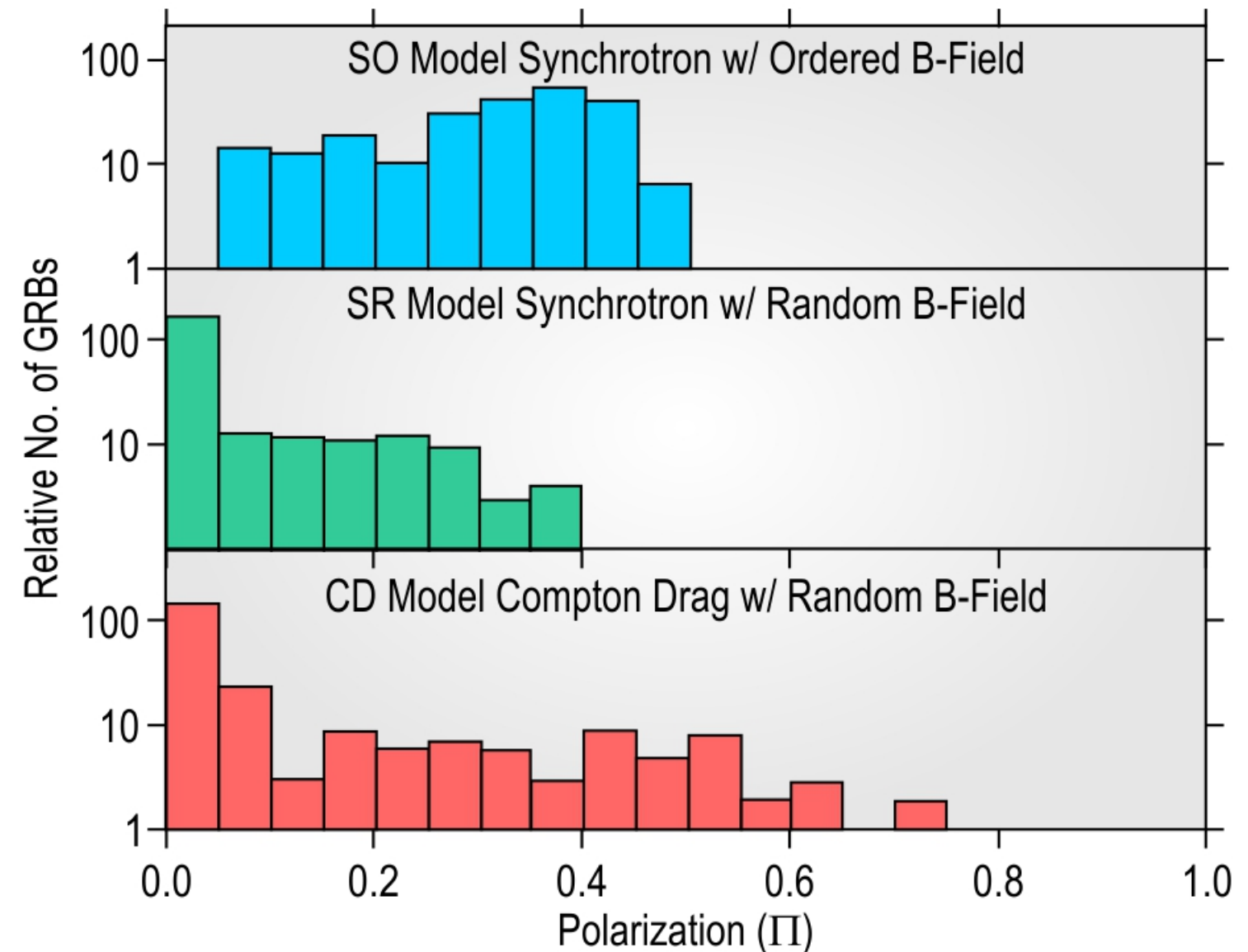
Emission Mechanism

- thermal blackbody
- synchrotron
- inverse Compton

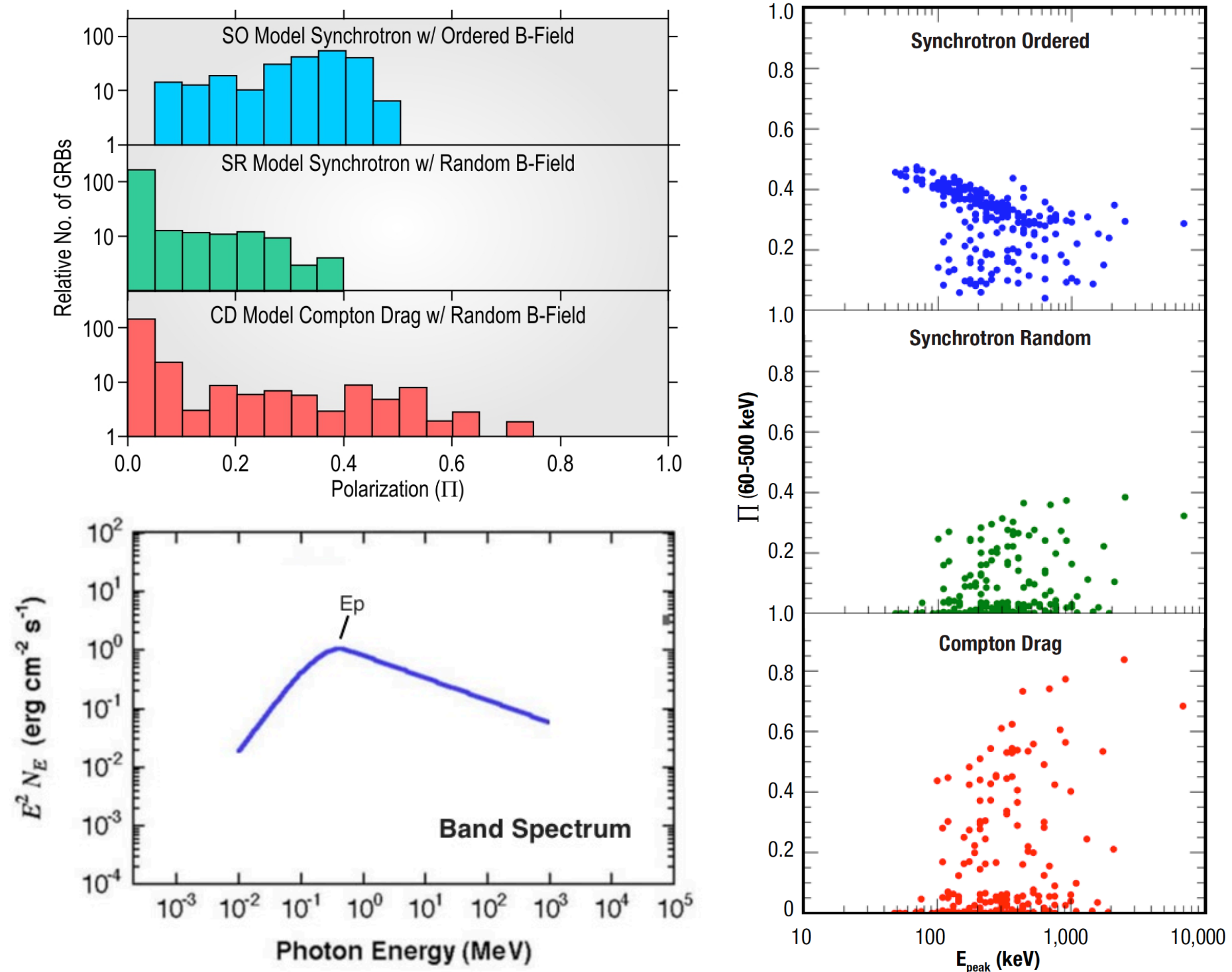
Gamma-Ray Bursts

- low polarization \Rightarrow randomly oriented B-fields \Rightarrow internal shocks \Rightarrow matter dominated
- high polarization \Rightarrow ordered B-fields \Rightarrow reconnection \Rightarrow Poynting flux

	Intrinsic Model	Geometric Models	
Objectives	Synchrotron Ordered	Compton Drag	Synchrotron Random
1. Magnetic Field	Ordered	Random	Random
2. Jet Composition	Poynting Flux	Matter	Matter
3. Jet Energy Dissipation Mechanism	Reconnection	Internal Shocks	Internal Shocks
4. Prompt Emission Mechanism	Synchrotron	Inverse Compton	Synchrotron
Predicted Polarization Properties (30-500 keV)			
Π distribution	peaks near 40%	peaks near 0%	peaks near 0%
Π maximum	60%	85%	40%
Fraction with $\Pi > 30\%$	62%	17%	2%



Gamma-Ray Bursts



The one dimensional polarization distributions can be expanded to two dimensions by using the E_p value for each GRB.

The resulting distributions can be used to further characterize each model.

GRB Polarization Measurements

Several results suggest very high polarization levels, but all are of limited statistical significance.

<i>Event</i>	<i>Mission</i>	<i>Energy (keV)</i>	<i>Result</i>	<i>Reference</i>
GRB 930131	CGRO/BATSE	20 - 1000	(35-100%)	Willis et al. (2005)
GRB 960924	CGRO/BATSE	20 - 1000	(50-100%)	Willis et al. (2005)
GRB 021206	RHESSI	150 - 2000	80% \pm 20%	Coburn & Boggs (2003)
GRB 041219a	INTEGRAL/SPI	100 - 350	98% \pm 33%	Kalemci et al. (2007)
GRB 041219a	INTEGRAL/SPI	100 - 350	96% \pm 40%	McGlynn et al. (2007)
GRB 041219a	INTEGRAL/IBIS	200 - 800	43% \pm 25% (variable π)	Götz et al. (2009)
GRB 061122	INTEGRAL/IBIS	250 - 800	> 60%	Götz et al. 2013
GRB 100826a	IKAROS/GAP	70 - 300	27% \pm 11% (variable PA)	Yonetoku et al. (2011)
GRB 110301a	IKAROS/GAP	70 - 300	70% \pm 22%	Yonetoku et al. (2012)
GRB 110721a	IKAROS/GAP	70 - 300	80% \pm 22%	Yonetoku et al. (2012)
GRB 140206a	INTEGRAL/IBIS	200 - 800	> 48%	Götz et al. (2014)

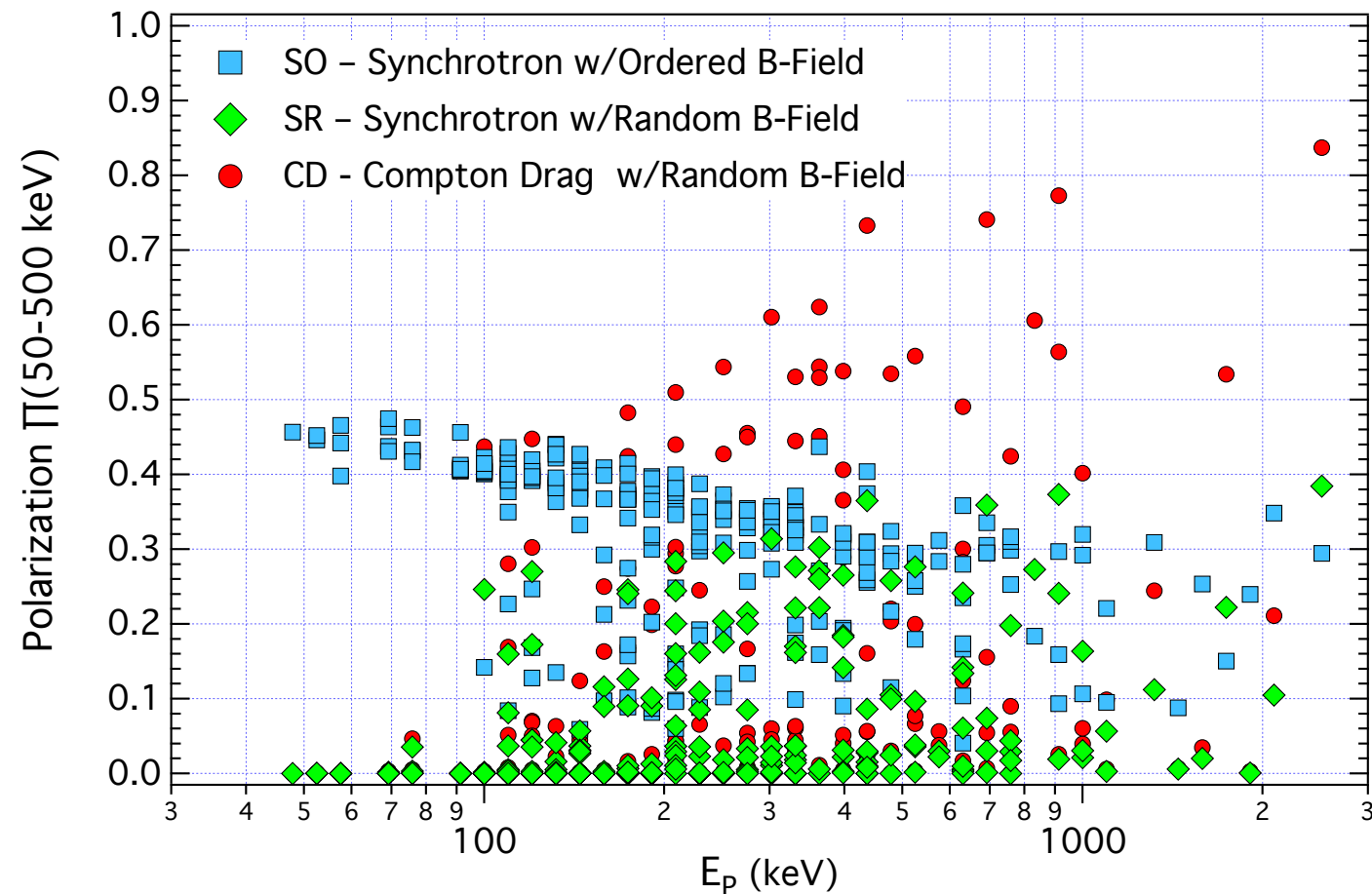
GRBs Measured by AstroSat-CZTI

GRB Name	Compton events	PF (%)	PA (°)	Chance Probability (%)
GRB 151006A	459	<79.2 ($\alpha = 0.05, \beta = 0.5$)	-	4.17
GRB 160106A	950	68.5 ± 24	$-22.5 \pm 12.0^\circ$	3.60
GRB 160131A	724	94 ± 31	$41.2 \pm 5.0^\circ$	<0.1
GRB 160325A	835	58.75 ± 23.5	$10.9 \pm 17.0^\circ$	5.00
GRB 160509A	460	96 ± 40	$-28.6 \pm 11.0^\circ$	<0.1
GRB 160607A	447	<75 ($\alpha = 0.05, \beta = 0.5$)	-	11.15
GRB 160623A	1400	<46.4 ($\alpha = 0.05, \beta = 0.5$)	-	49.05
		<57.1 ($\alpha = 0.01, \beta = 0.5$)		
GRB 160703A	448	<54.5 ($\alpha = 0.05, \beta = 0.5$)	-	0.68
		<68.1 ($\alpha = 0.01, \beta = 0.5$)	-	
GRB 160802A	901	85 ± 29	$-36.1 \pm 4.6^\circ$	<0.1
GRB 160821A	2549	48.7 ± 14.6	$-34.0 \pm 5.0^\circ$	<0.1
GRB 160910A	832	93.7 ± 30.92	$43.5 \pm 4.0^\circ$	<0.1

Chattopadhyay et al. (2017)

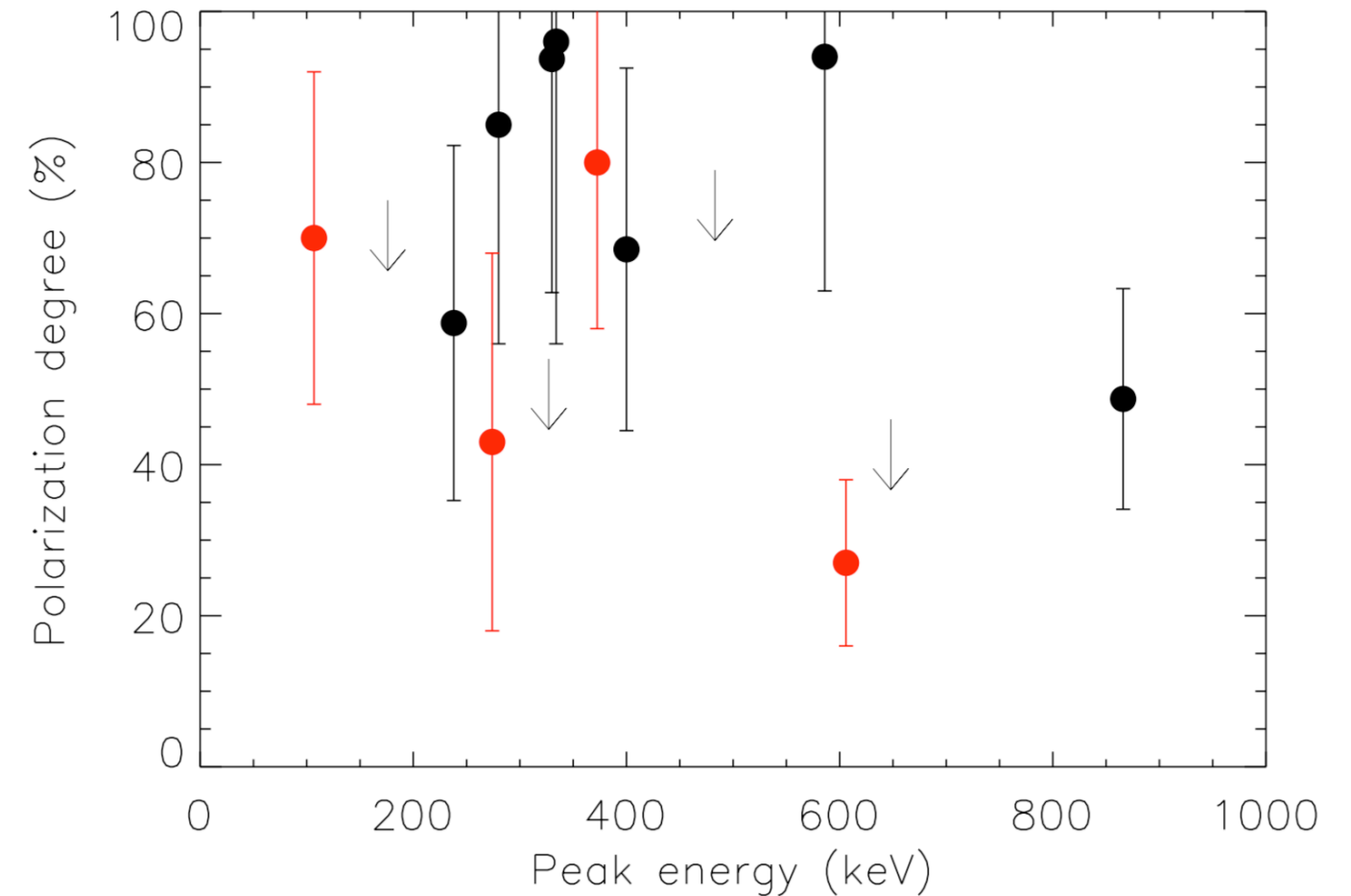
GRB Polarimetry

Polarization fraction as a function of E_p for various general classes of GRB models. The distribution of measured GRBs in this data space can be used to constrain GRB physics.



Toma et al. (2008)

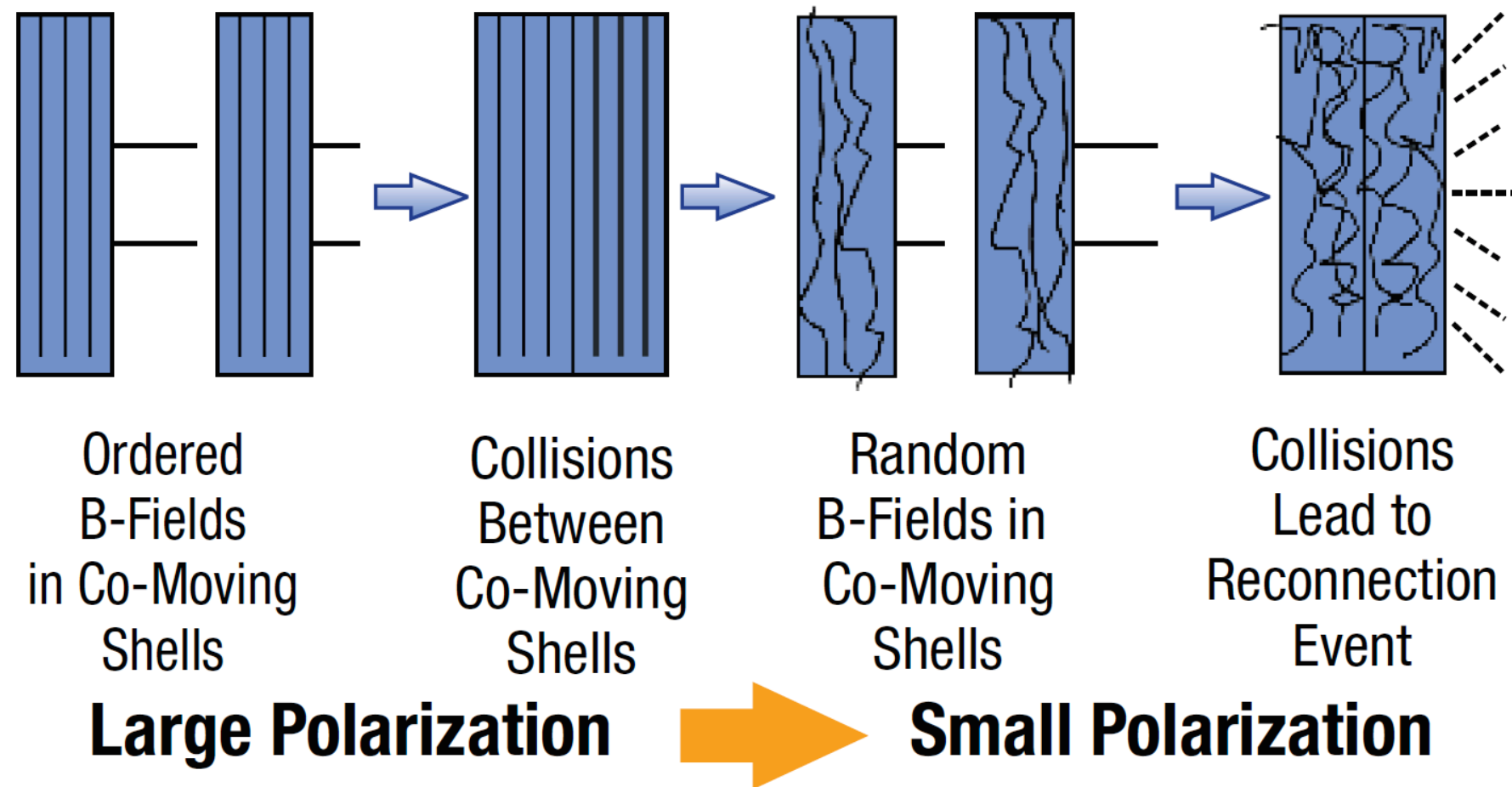
Polarization fraction as a function of E_p for the GRBs for which polarizations have been estimated. The black points are from AstroSat-CZTI. The red points are from GAP and INTEGRAL.



Chattopadhyay et al. (2017)

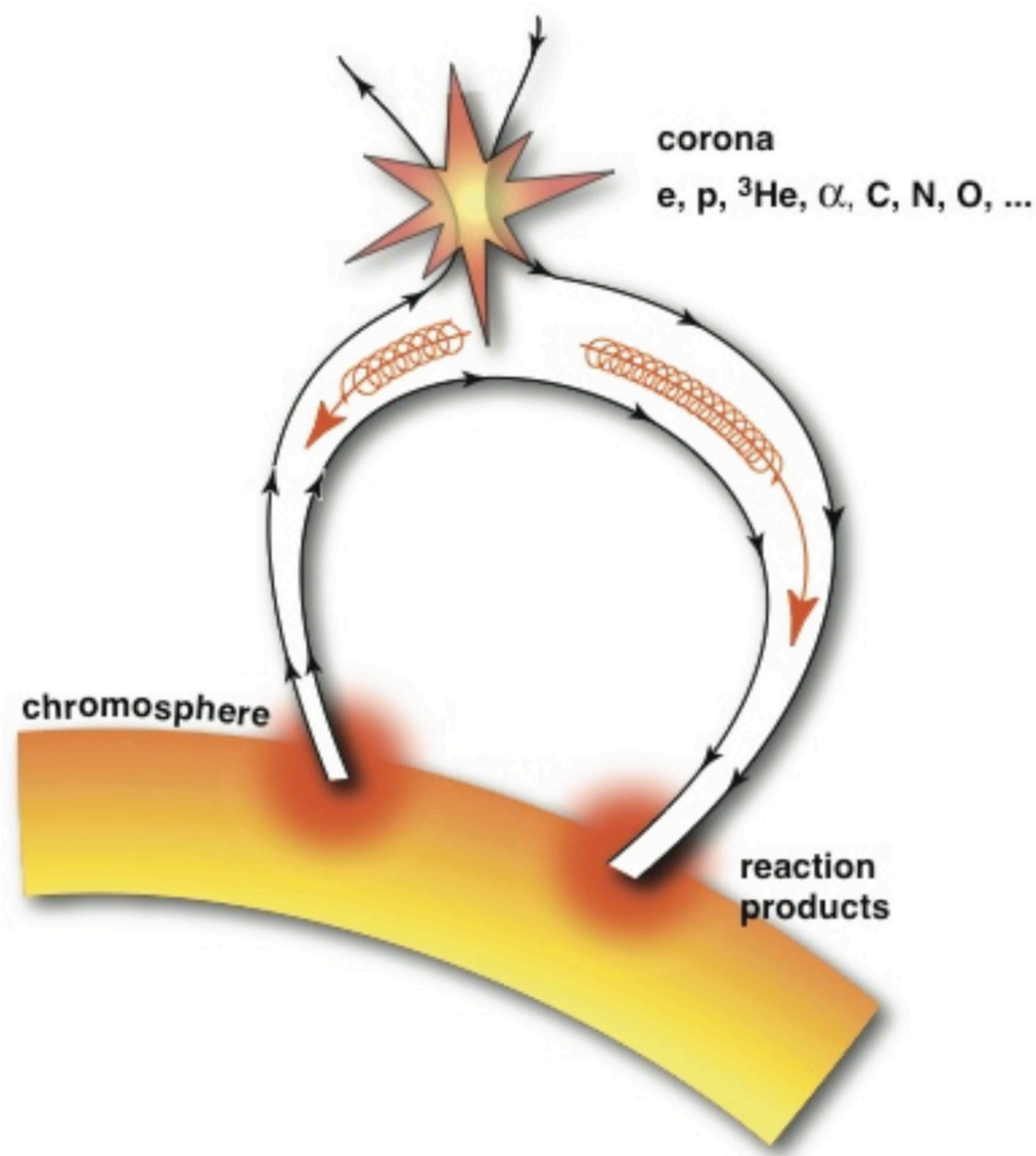
Time Variable GRB Polarization

In the Internal-Collision induced MAgnetic Reconnection and Turbulence (ICMART) model of GRBs (Zhang and Yan, 2011), each broad pulse in the GRB light curve is related to one event that destroys the ordered magnetic fields through reconnection to produce radiation. In this case, a decrease of the polarization with time is expected across each broad pulse, as the field structure evolves from order to disordered.

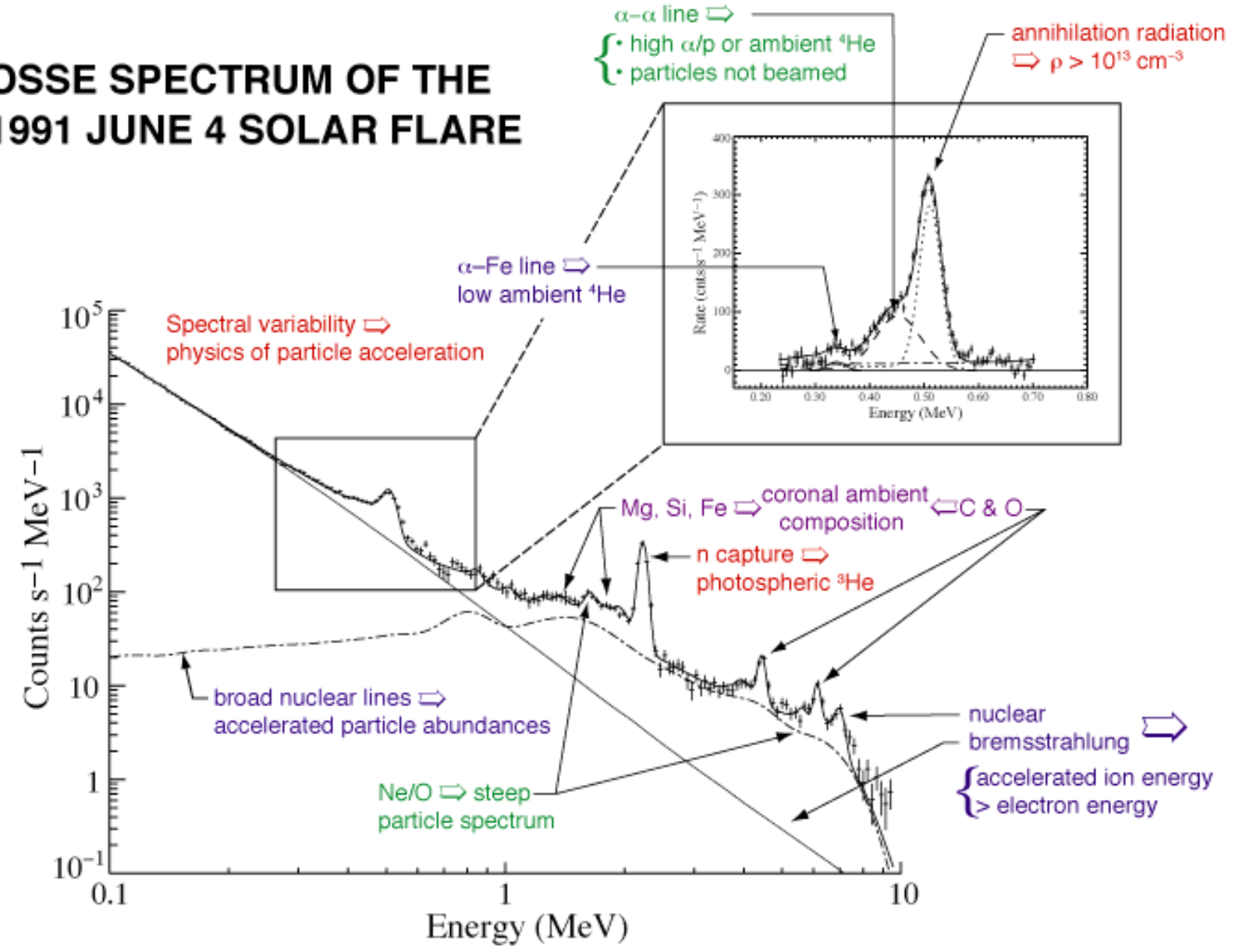


Solar Flares

Polarized emission may come from the non-thermal electron bremsstrahlung.
 Bremsstrahlung polarization is parallel to the acceleration vector of the electron.
 Can be used to constrain the accelerated electron pitch angle distribution (electron beaming).

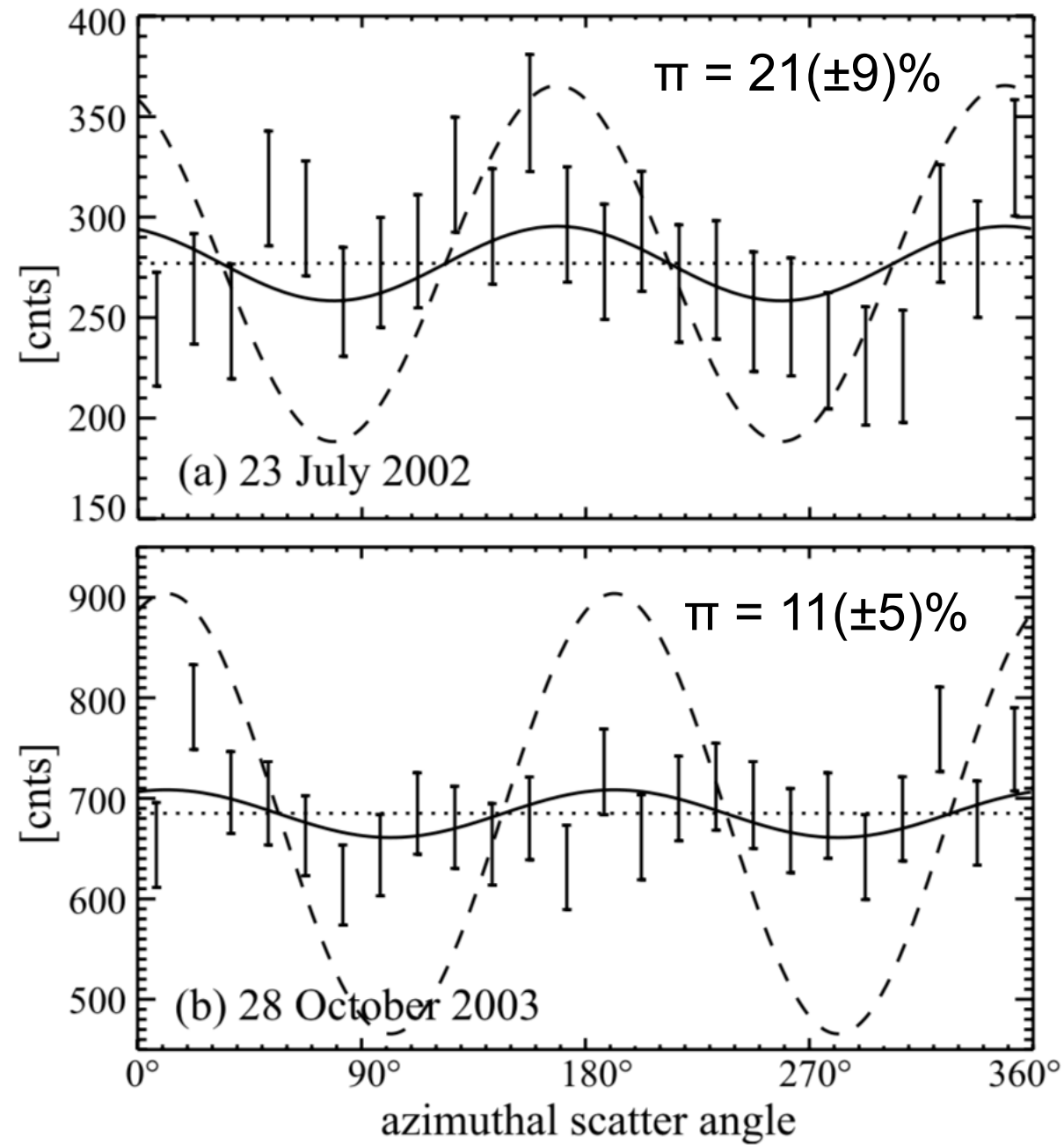


OSSE SPECTRUM OF THE 1991 JUNE 4 SOLAR FLARE



Solar Flare Measurements

RHESSI – 200-1000 keV

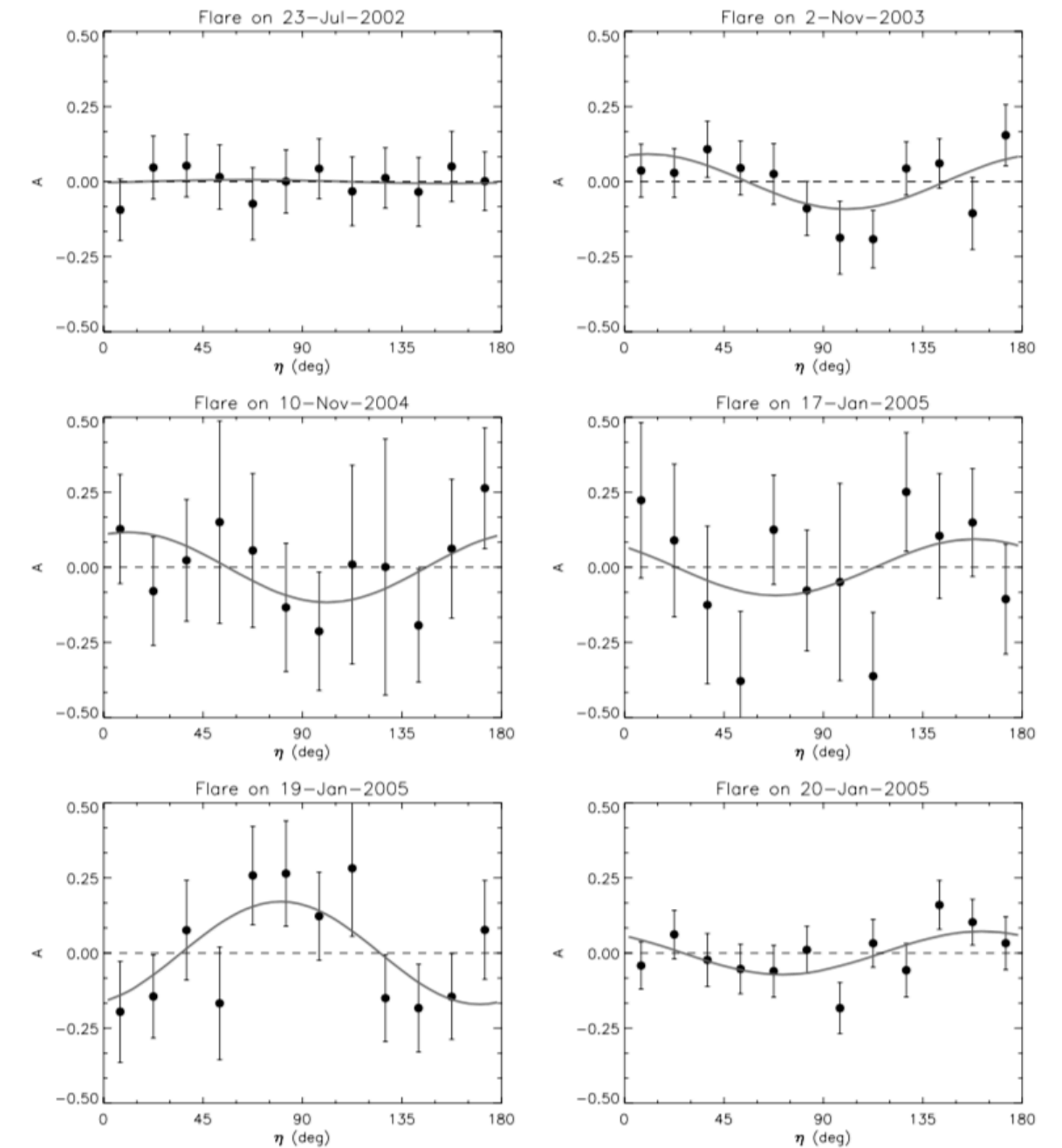


Boggs et al. 2006



RHESSI Ge array has been used for flare polarization measurements.

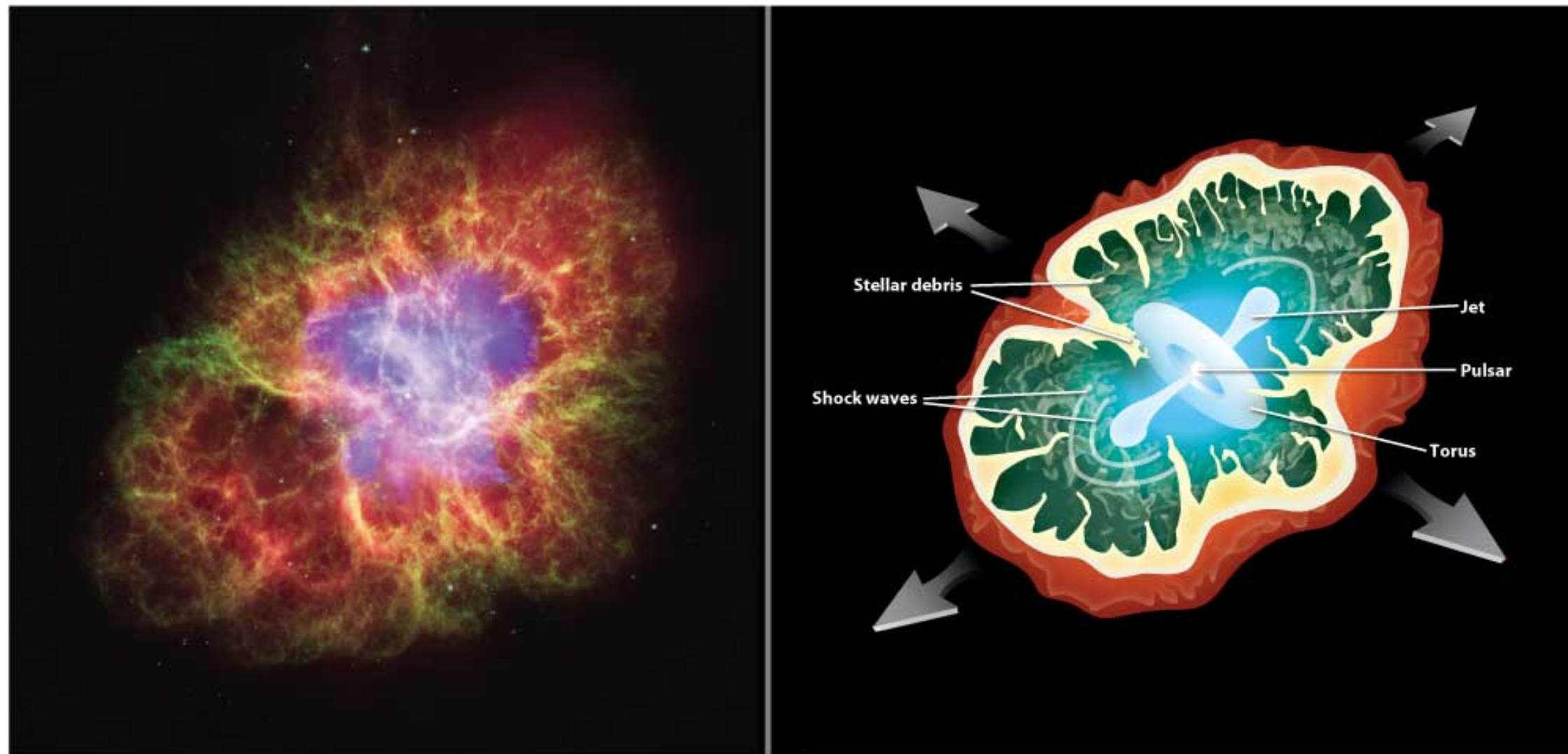
RHESSI – 100-350 keV



Suarez-Garcia et al. 2006

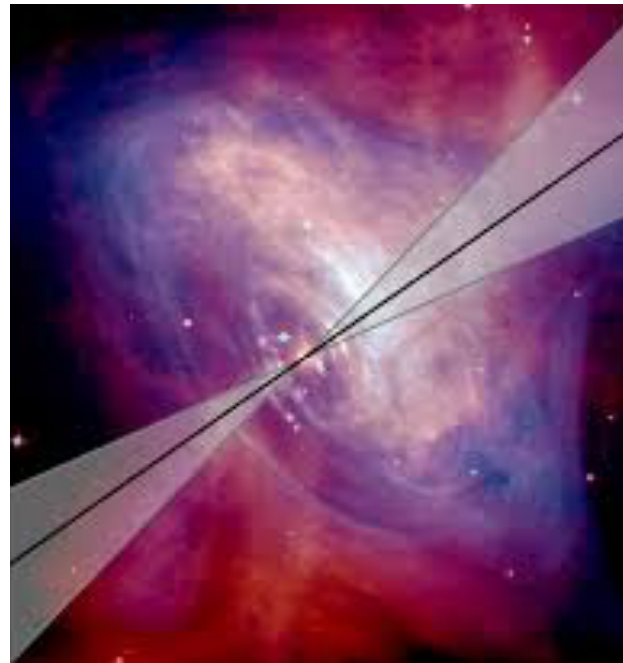
Crab Pulsar / Nebula

33 ms pulsar accelerates particles up to $\sim 10^{15}$ eV.
At MeV energies, emission is dominated by synchrotron.
At higher energies, inverse Compton appears to dominate.

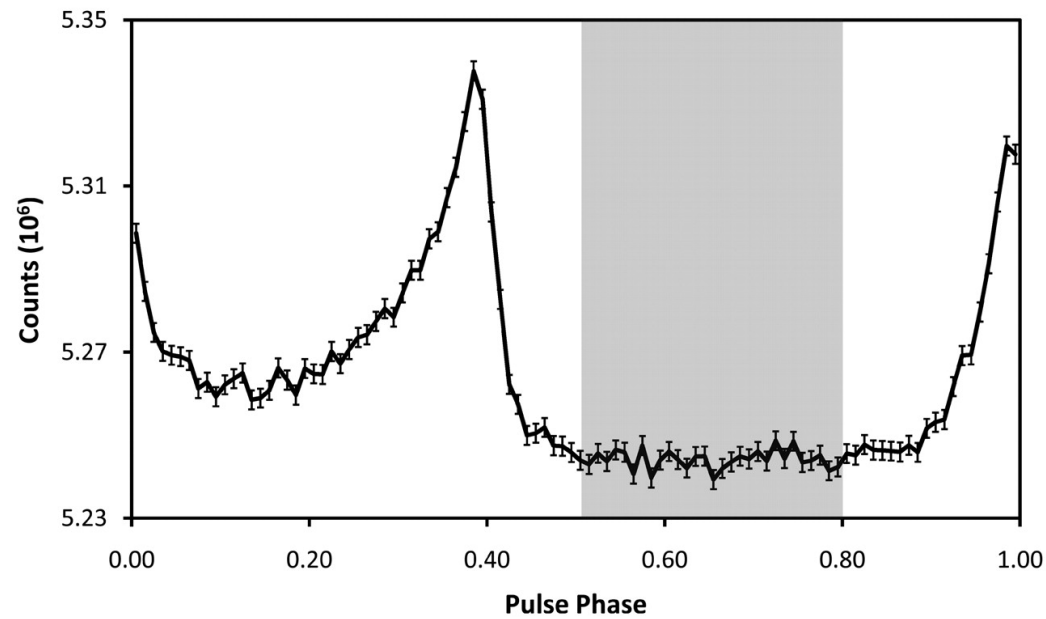


Crab Polarization - INTEGRAL

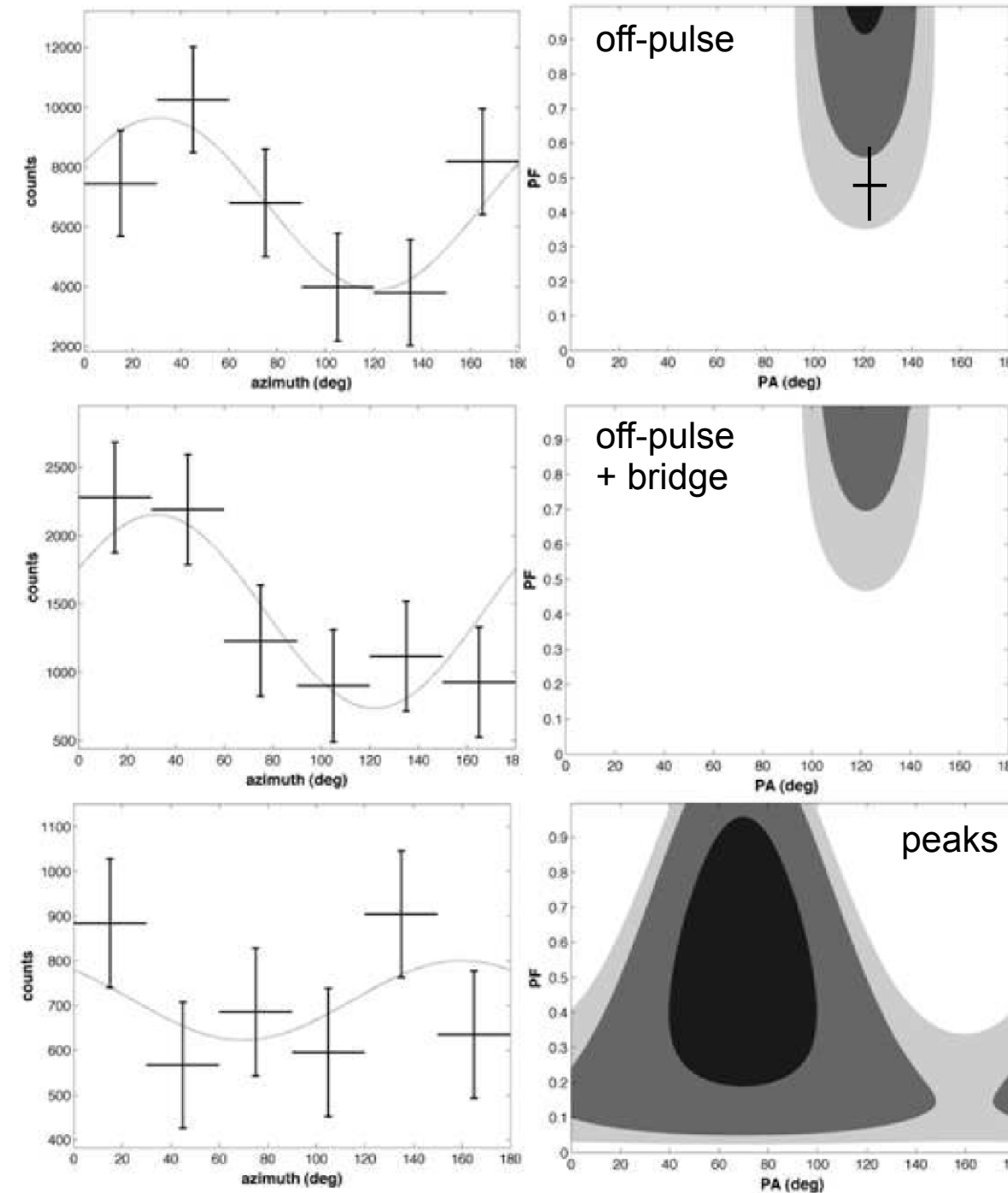
INTEGRAL/SPI – 100 keV - 1 MeV
Dean et al. 2008



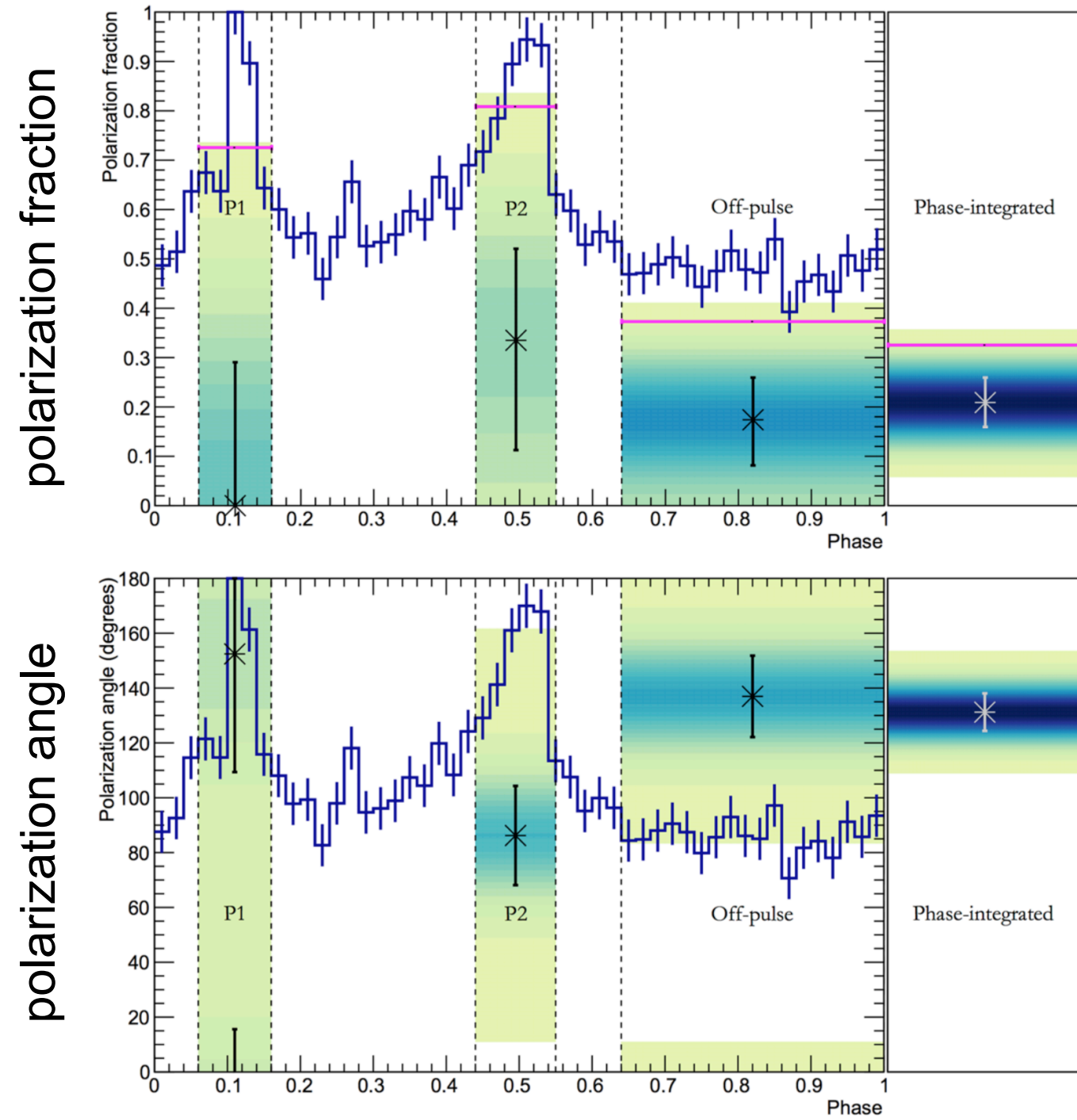
$\pi = 46(\pm 10)\%$
off-pulse
aligned with
rotation axis



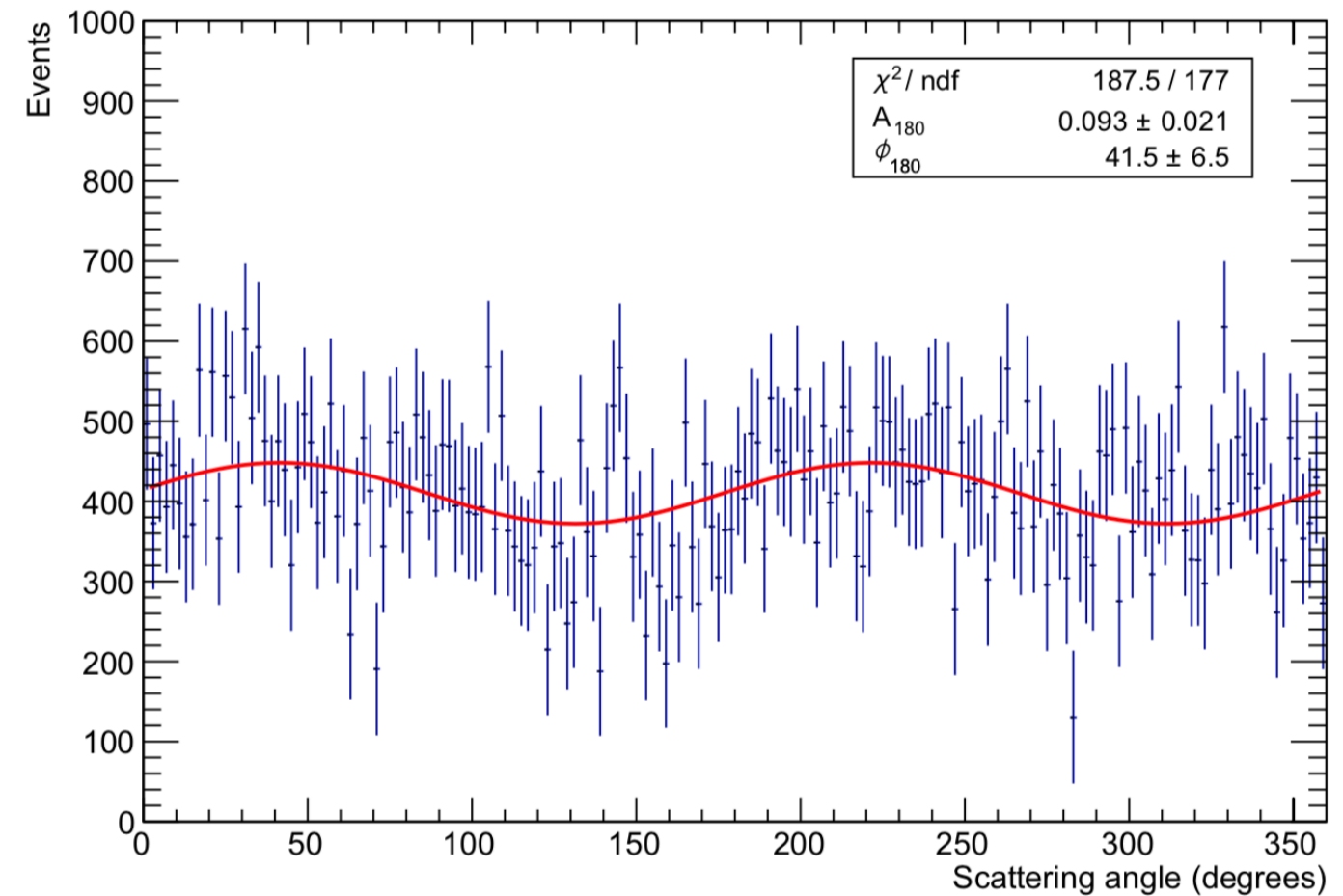
INTEGRAL/IBIS – 200 - 800 keV
Forot et al. 2008



Crab Polarization - PoGO+



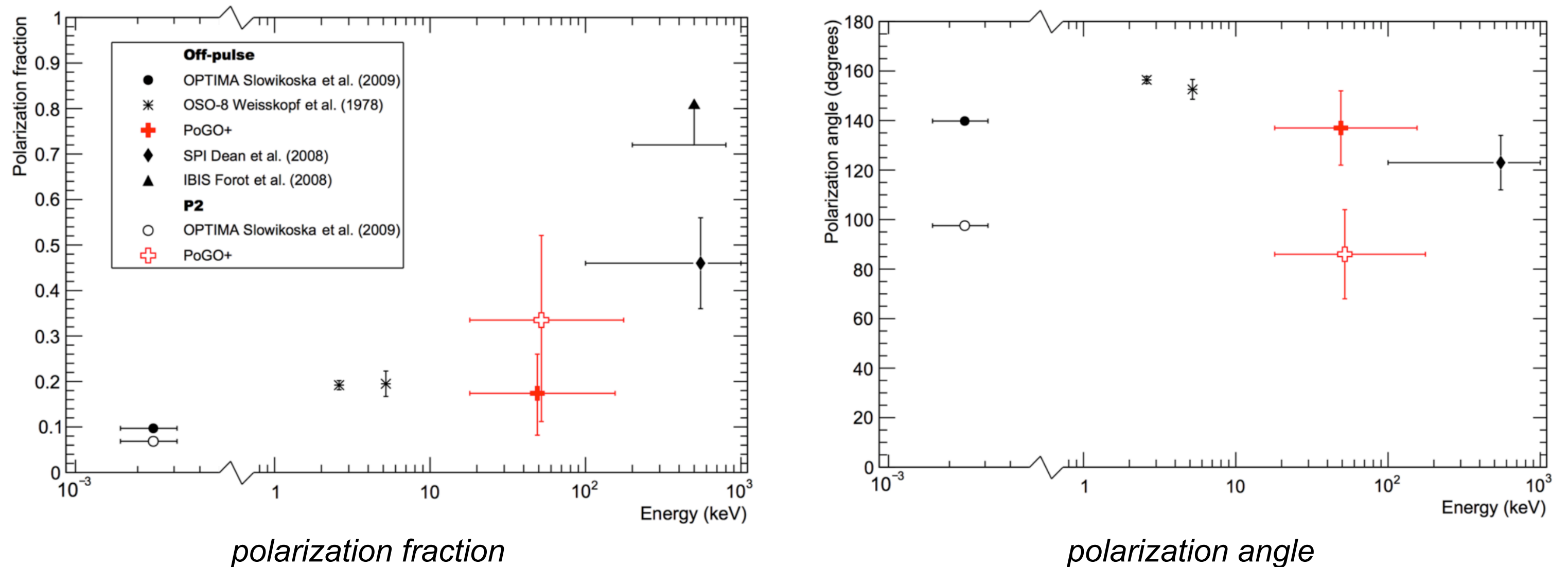
Balloon measurements from 20-160 keV.
 Lower polarization values than INTEGRAL,
 but aligned with rotation axis.



Chauvin et al. (2017)

Energy-Dependence

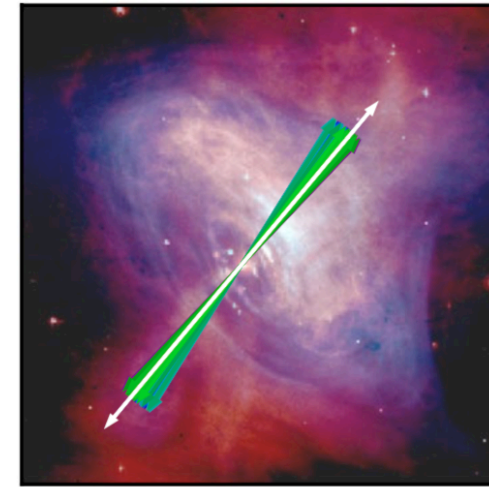
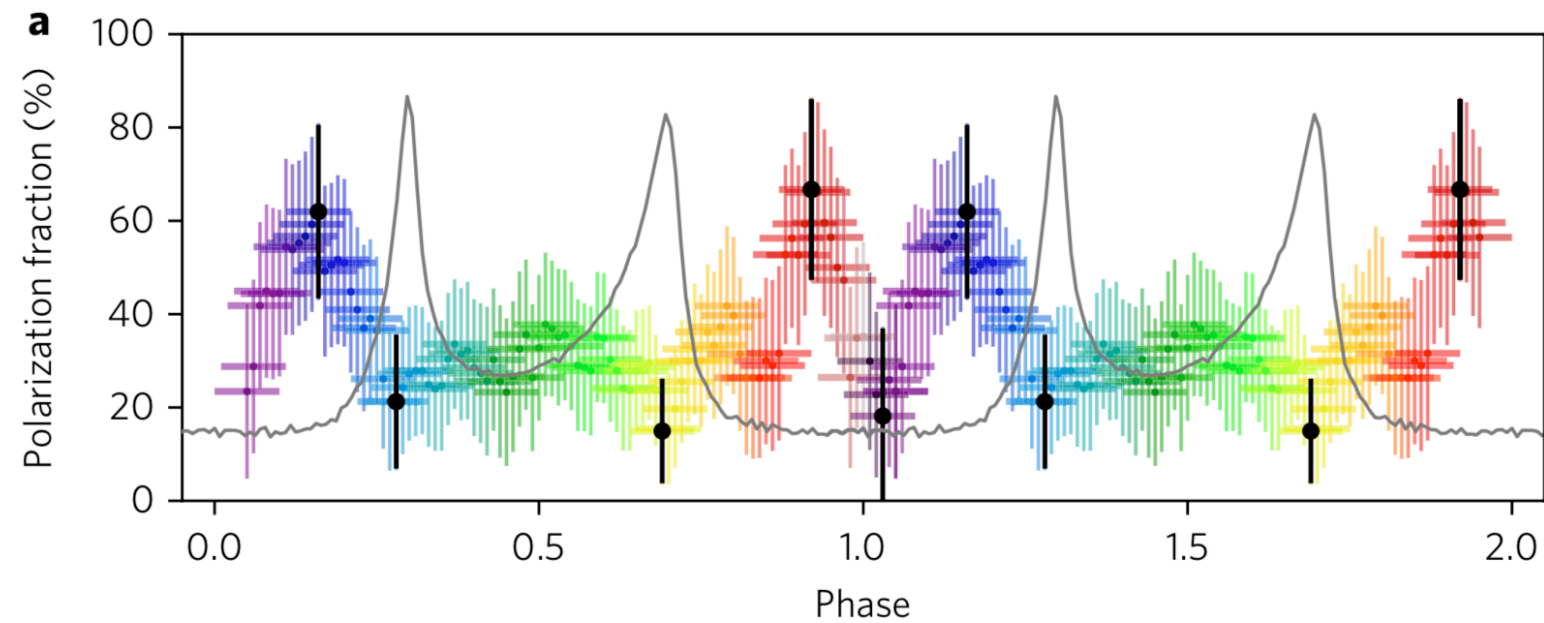
These data correspond to the off-pulse signal.
Alignment of the polarization angle with the pulsar spin axis suggests an origin consistent with a toroidal magnetic field in the vicinity of the pulsar.



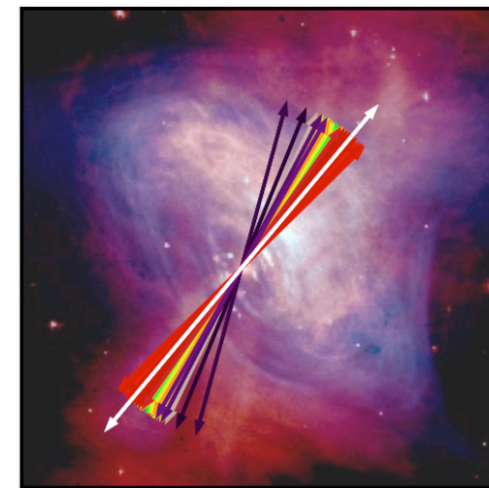
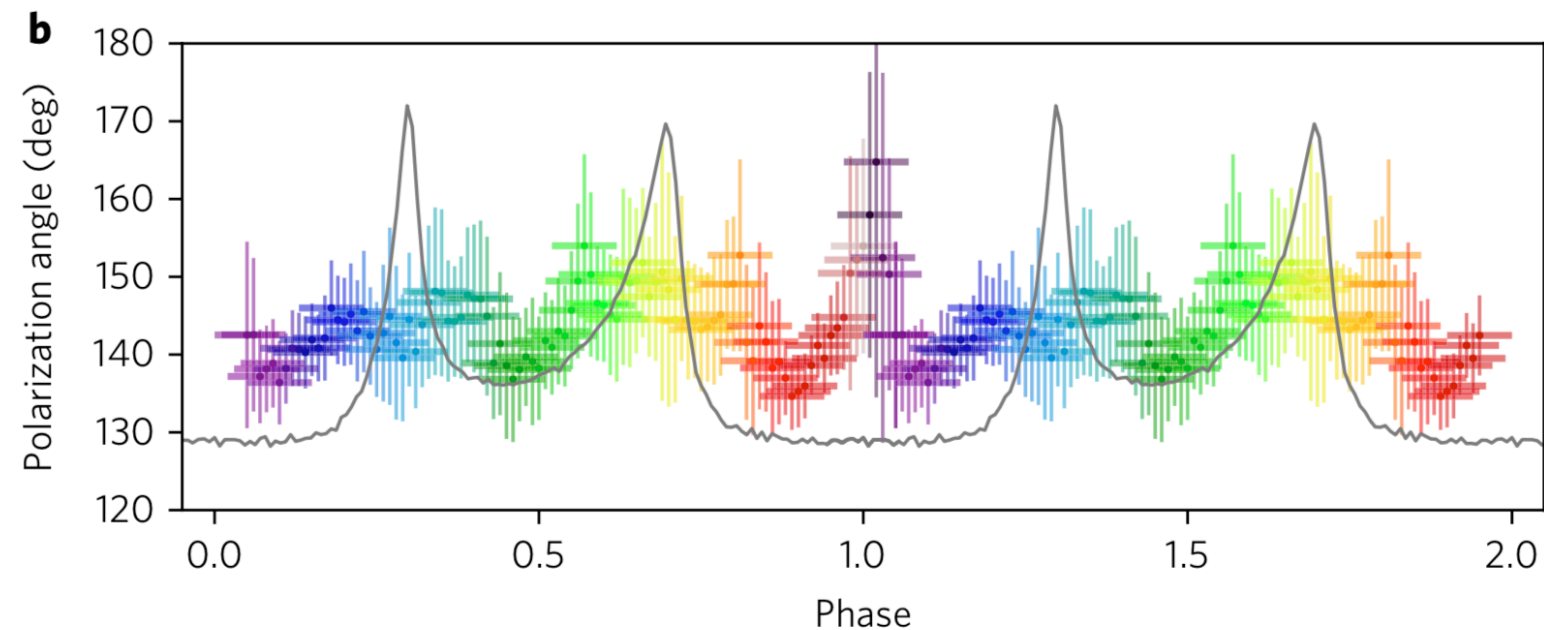
Chauvin et al. (2017)

Crab Polarization - AstroSat

Phase-resolved polarimetry using “dynamic binning” of 100-380 keV data.



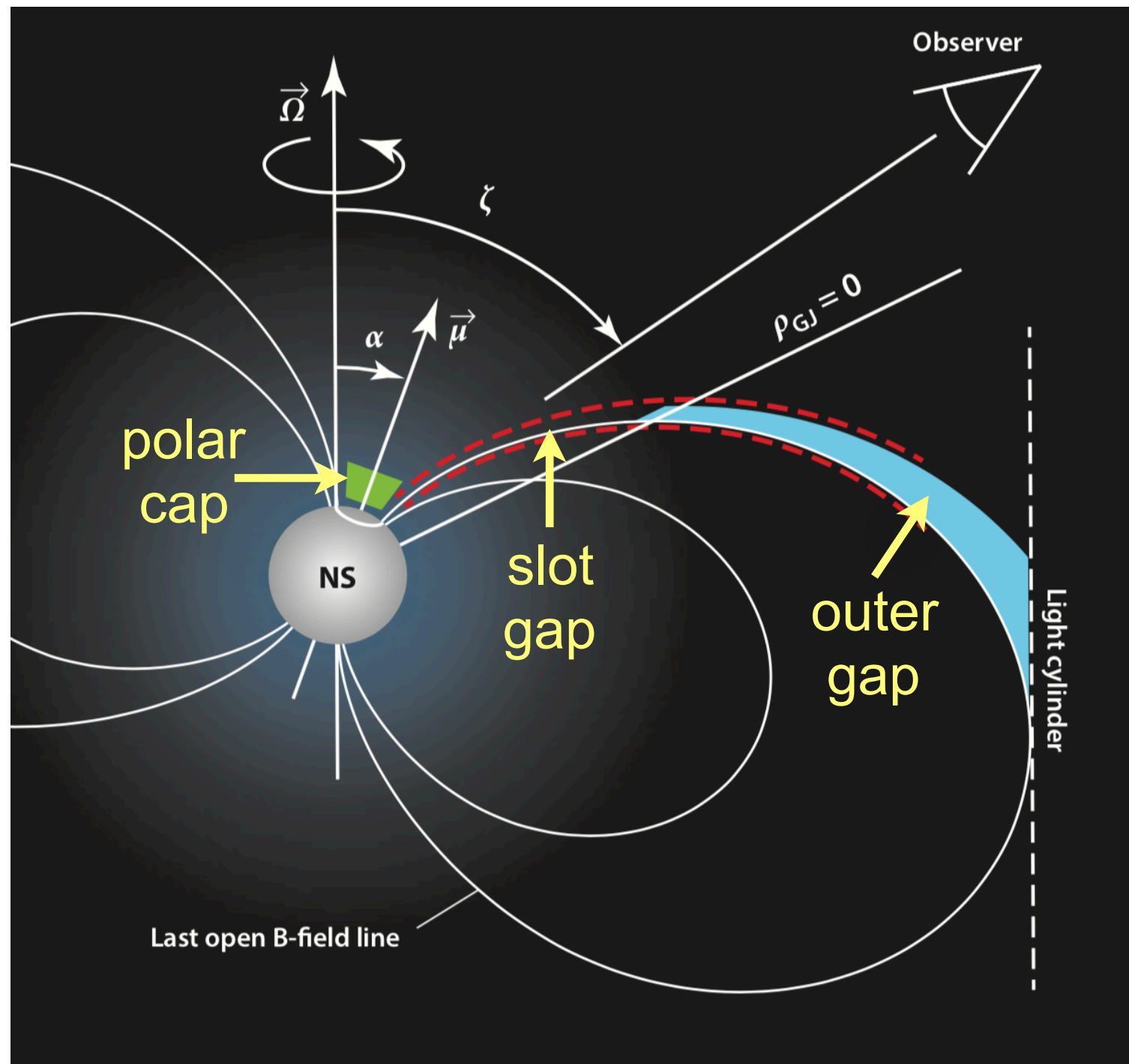
Data indicate higher polarization during off-pulse phase, with polarization angle aligned with rotation axis at all phases.



The variation in off-pulse polarization is difficult to understand with current models.

Vadawale et al. 2017

Rotation Powered Pulsars



Caraveo (2014)

The Crab is not the only pulsar visible at MeV energies. Many are not associated with nebular emission.

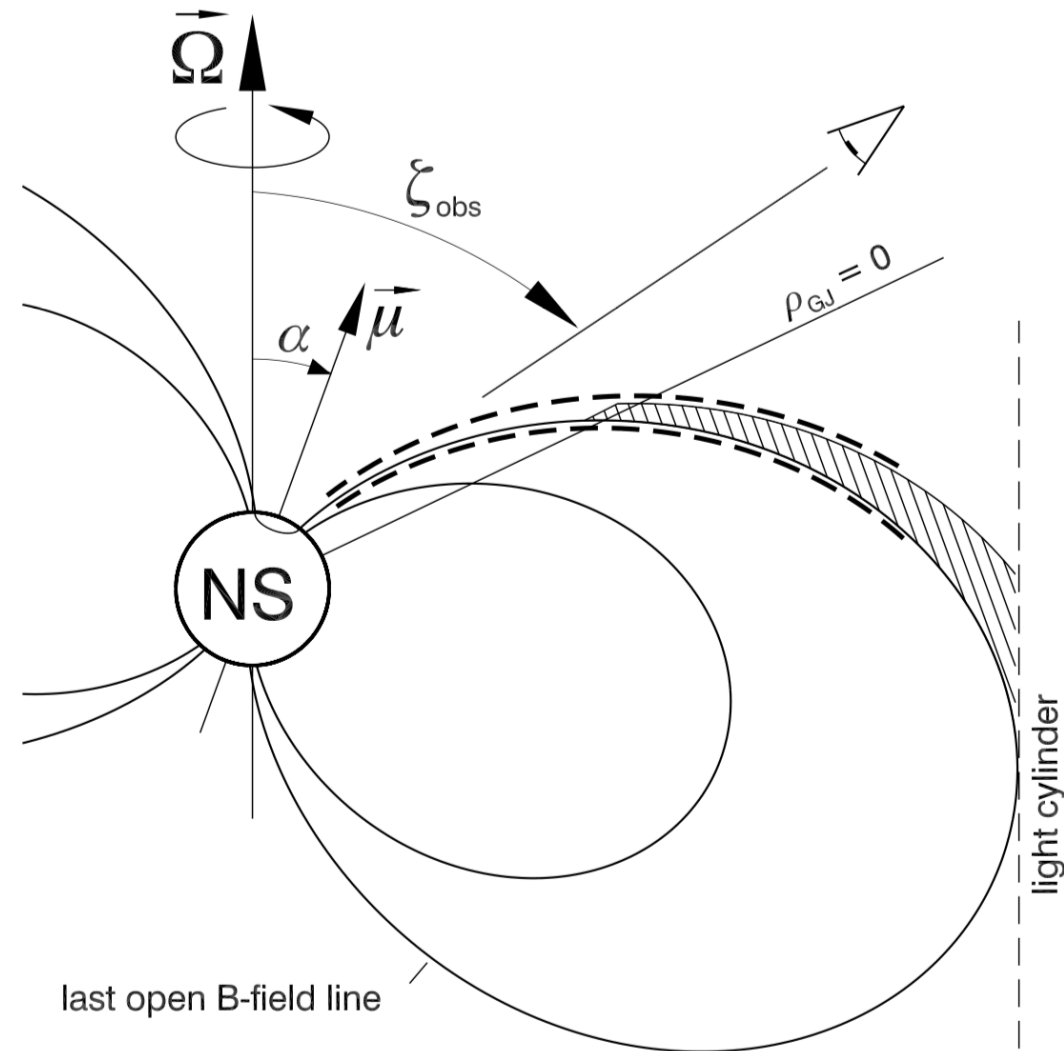
Most pulsar emission models invoke particle acceleration in one of three regions within the light cylinder.

Acceleration outside the light cylinder has also been suggested.

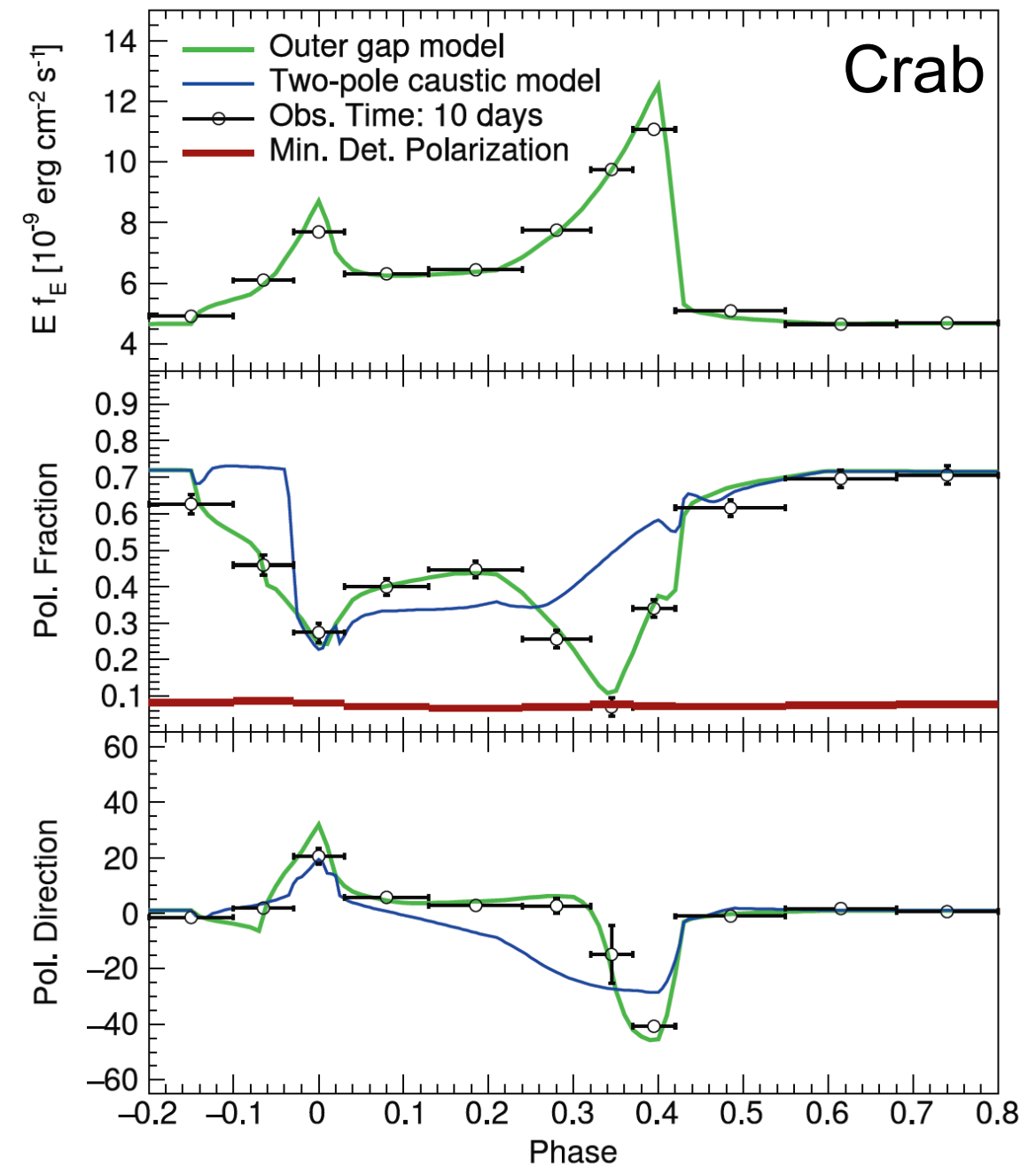
These different models predict different behavior of the γ -ray polarization as a function of pulse phase.

Acceleration Site

Observations with AMEGO should be able to distinguish between different models, in this case between the outer-gap model and the two-pole caustic (slot-gap) model.



Dyks & Rudak (2003)

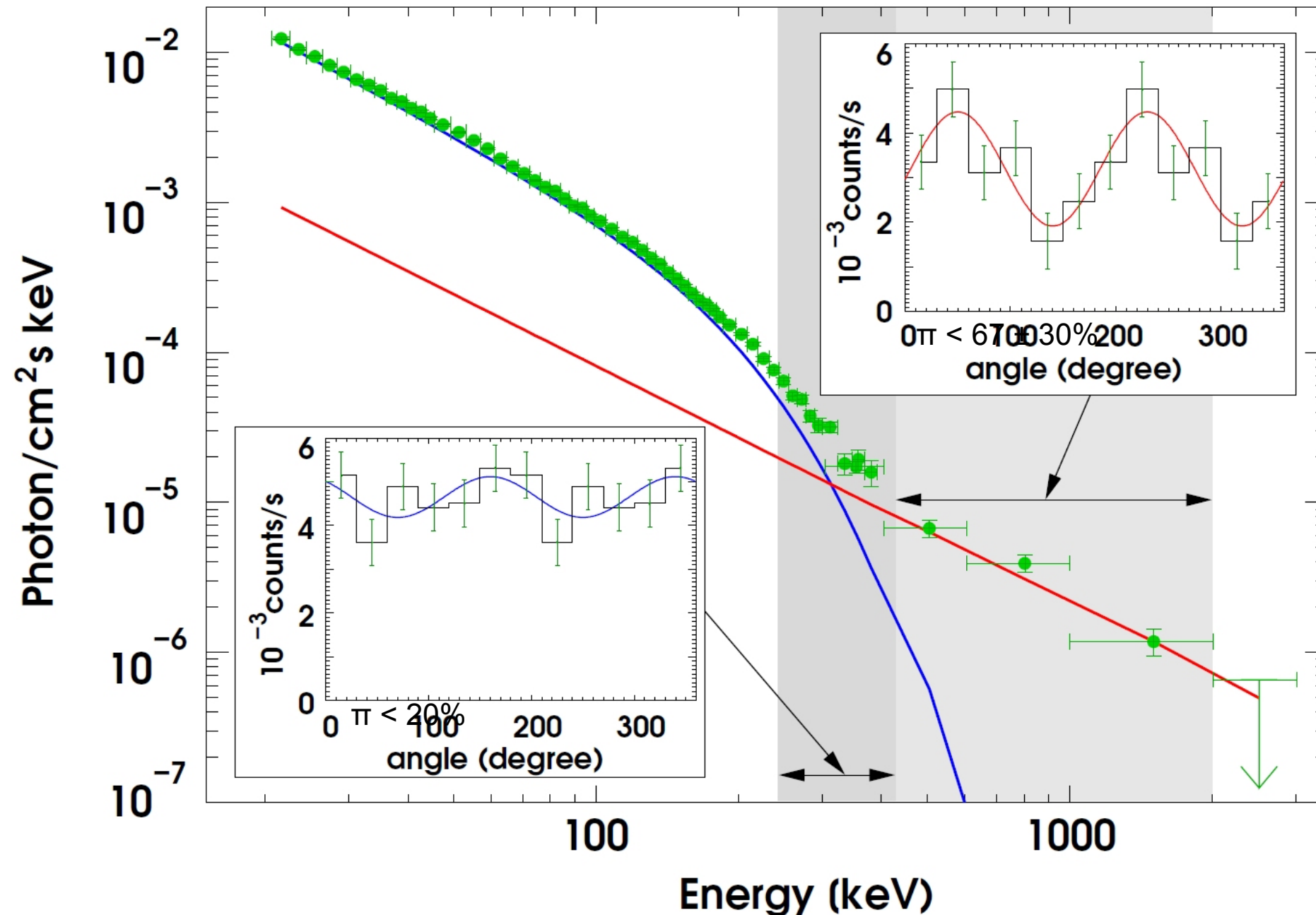


Kislat et al. (2017)

Dyks, Harding & Rudak (2004)

Cygnus X-1

INTEGRAL / IBIS



The IBIS results shown here are supported by similar results from SPI. We can disentangle the jet emission, which can be highly polarized, from the Compton scattering of disk photons on thermal electrons, which is expected to be only weakly polarized.

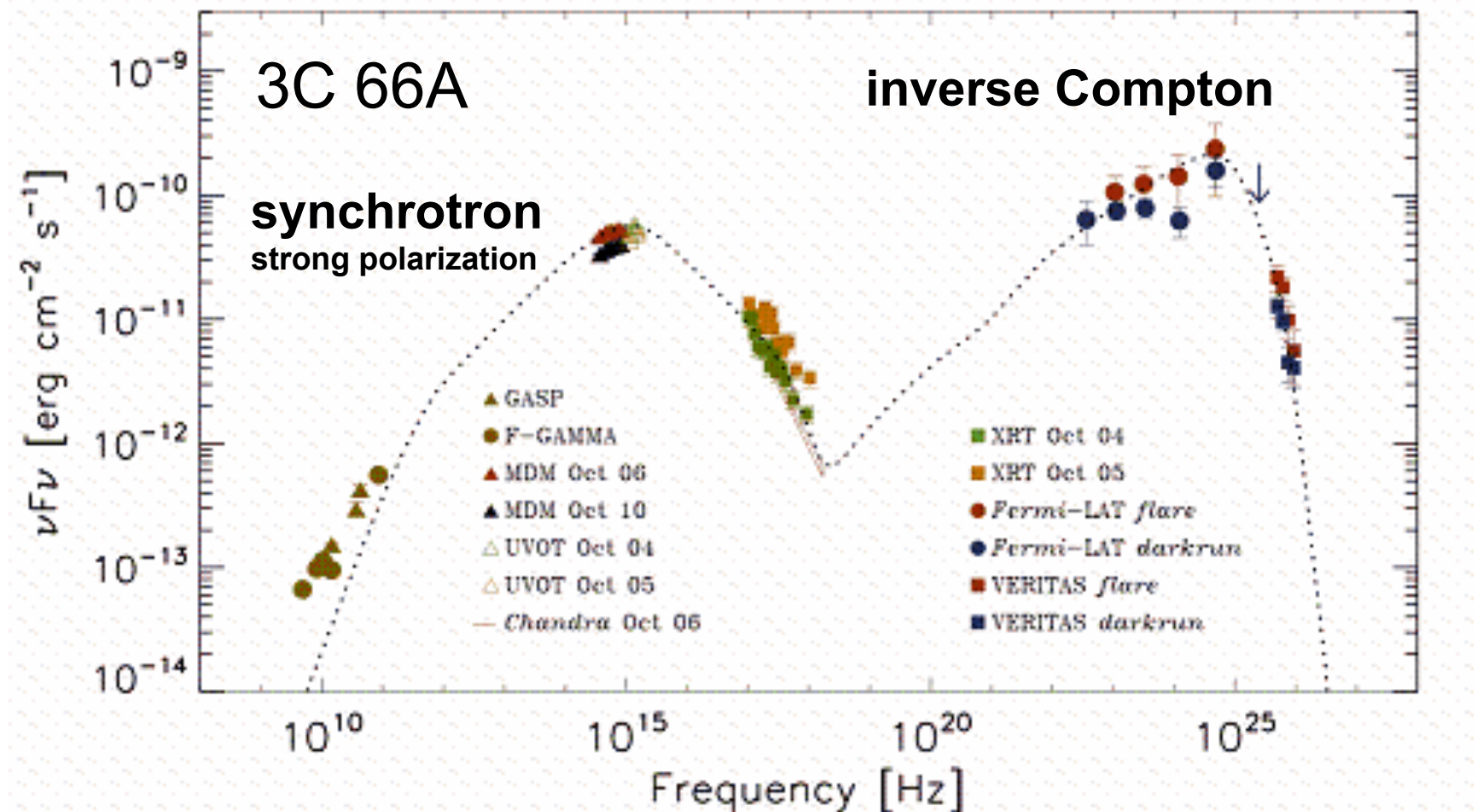
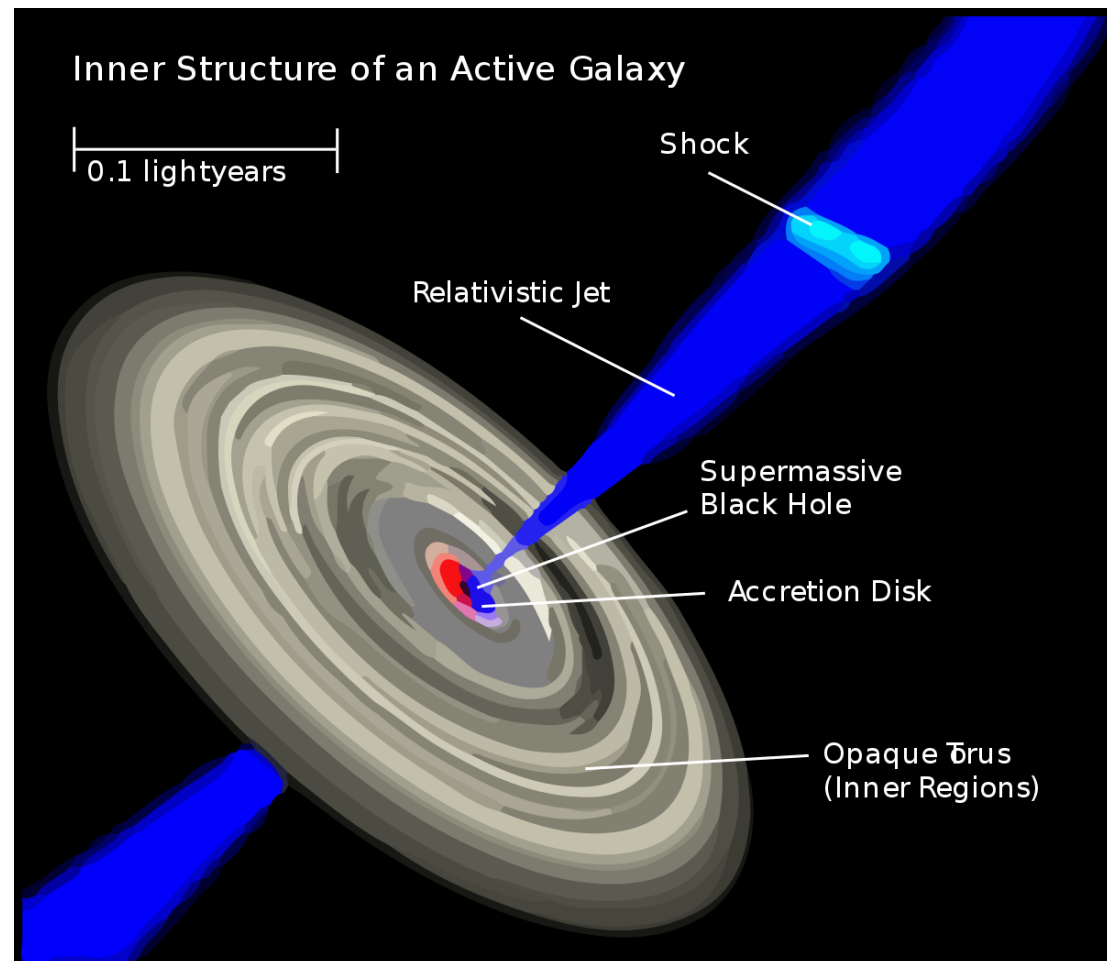
These results (stronger polarization at higher energies) provide additional evidence that the high-energy tail is likely associated with jet emission.

Laurent et al. 2011 (IBIS) / Jourdain et al. 2012 (SPI)

Blazars

Blazars are radio-loud AGN where the jet points at (or close to) our line of sight. Doppler-boosted jet radiation dominates the emission from the accretion disk.

Broadband spectra exhibits two peaks, one in mm- to soft X-ray band, one in gamma-ray band. Our knowledge of the gamma-ray peak is often incomplete, owing to a lack of sensitive coverage.



Blazars

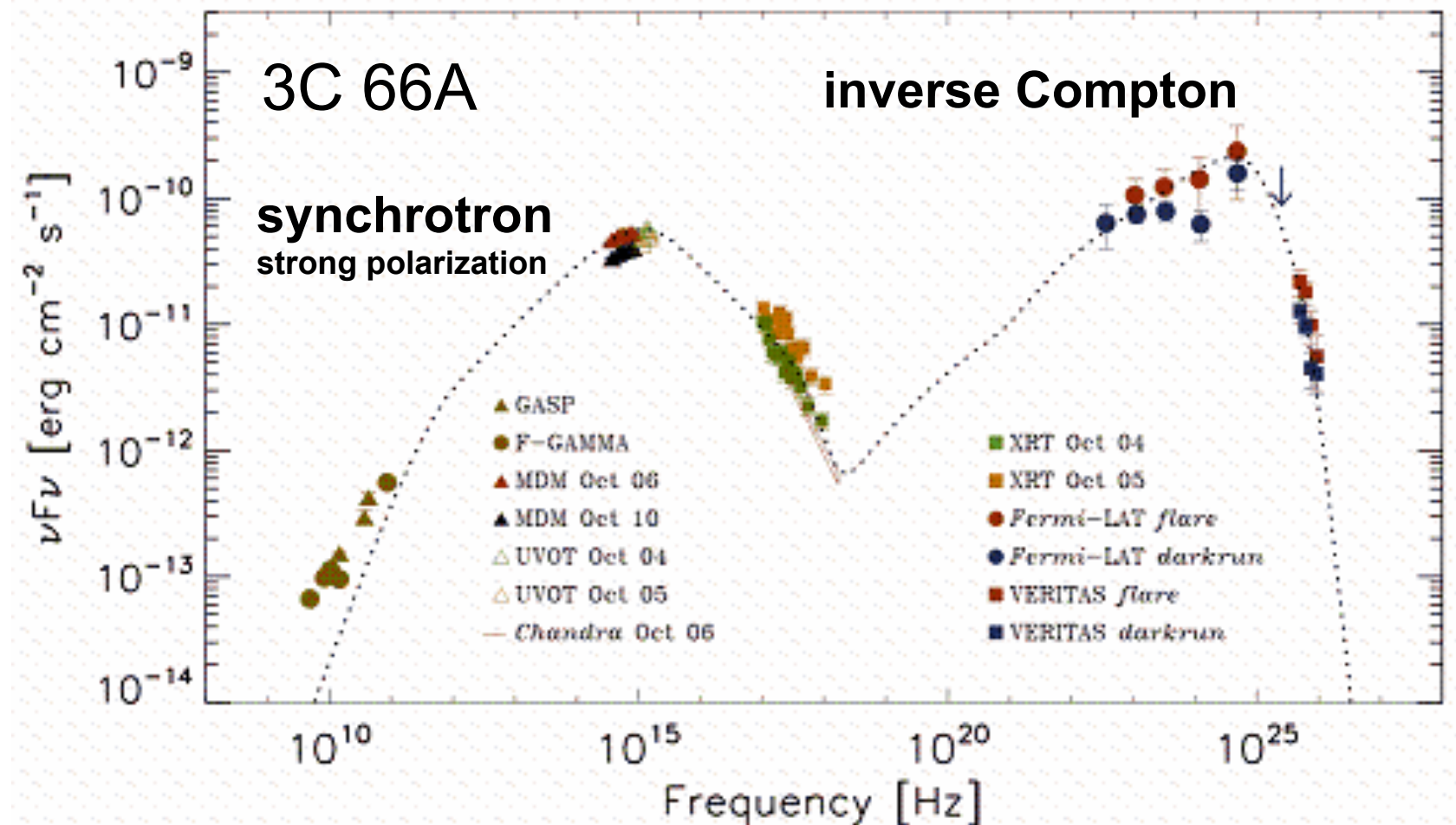
At MeV energies, the emission is expected to be from inverse Compton.

The origin of the seed photons is uncertain.

MeV polarization will depend on the origin (polarization) of the seed photons.

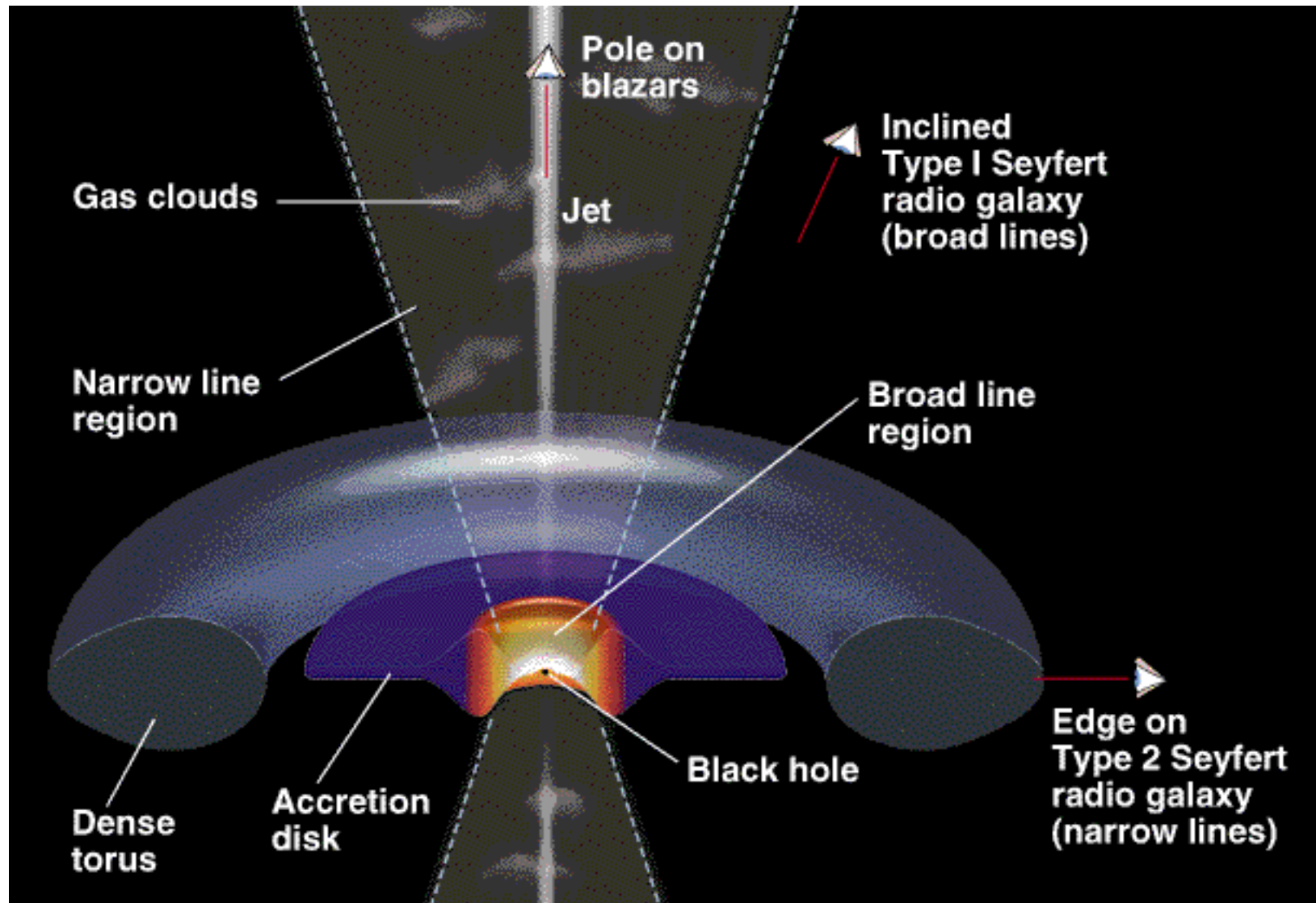
If seed photons are low energy radiation from the disk or torus, the seed photons are not expected to be polarized. The IC radiation will also not be polarized.

If seed photons are synchrotron radiation from the jet (SSC), the seed photons are likely to be polarized. The IC radiation will also be polarized.



Blazar Geometry

The gamma-rays come from inverse Compton emission generated by seed photons interacting with the energetic electrons in the jet.



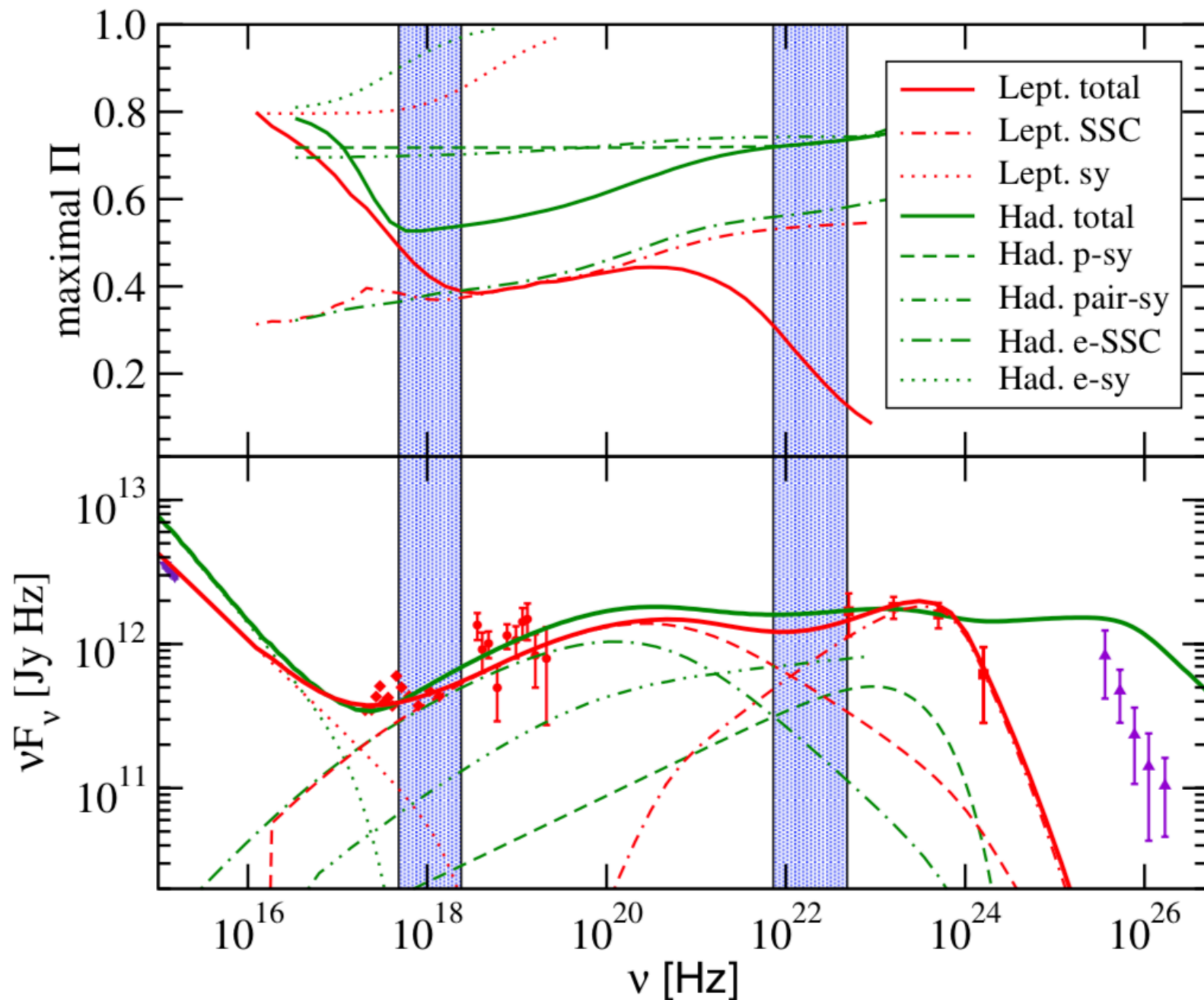
The polarization of the observed emission will indicate the origin of the seed photons (i.e., the emission geometry).

If the IC peak is polarized, then the seed photons are likely polarized, suggesting a jet origin for the seed photons.

If the IC peak is not polarized, then the seed photons are also likely unpolarized, suggesting an origin outside of the jet for the seed photons.

Leptonic vs. Hadronic Emission

BL Lacertae



Zhang & Böttcher (2013)

MeV polarimetry can also tell us about the jet composition, in particular whether the jet is largely leptonic or hadronic. Hadronic jets are expected to exhibit higher levels of polarization at MeV energies.

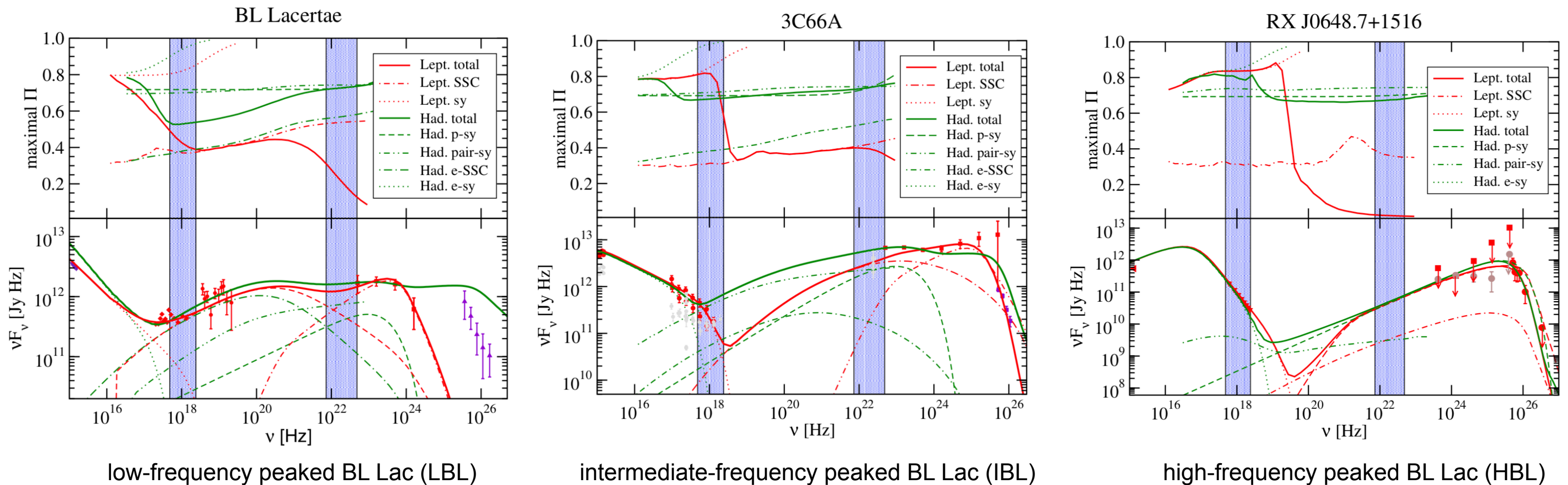
Zhang & Böttcher (2013) have modeled the polarization for a number of blazars that have been detected by Fermi.

Both leptonic and hadronic models can fit the observed spectra, but they make different predictions about the polarization as a function of energy.

Leptonic vs. Hadronic Emission

At X-ray energies, there is little difference in the polarization between leptonic and hadronic models.

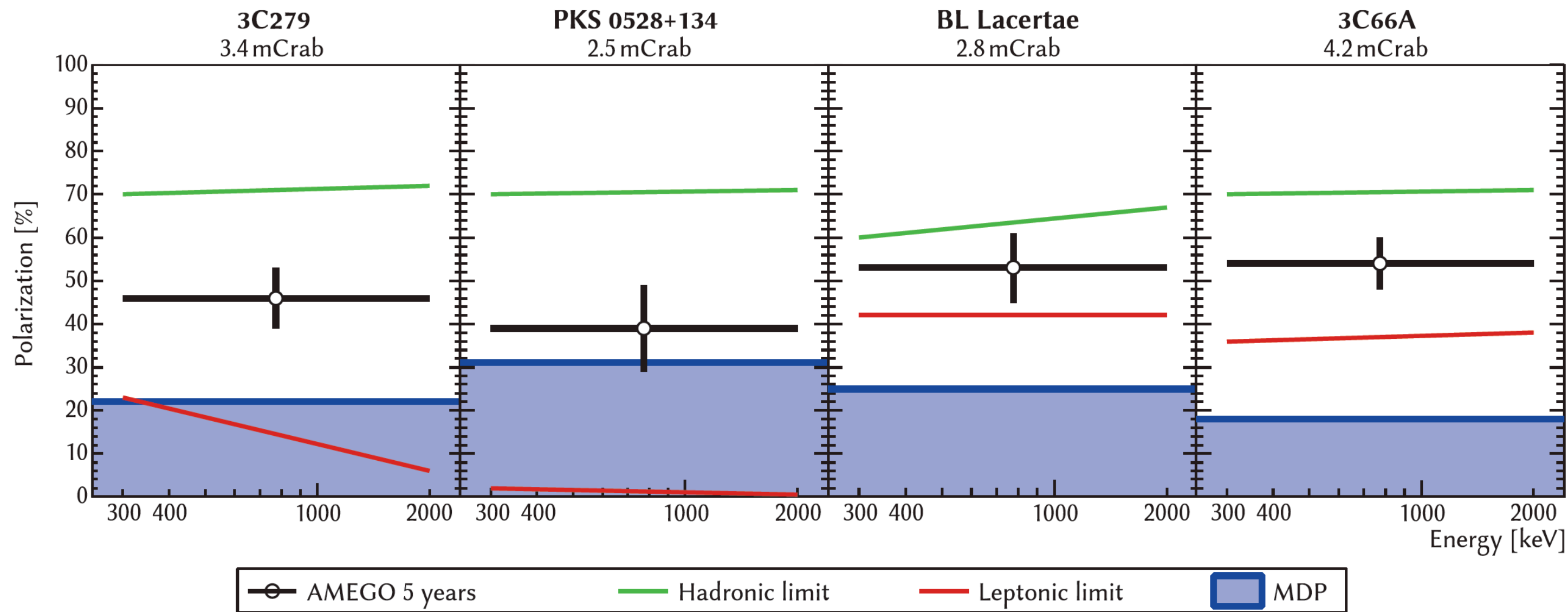
At higher energies, there is a significant difference, with the difference being larger for blazars that have a synchrotron component that peaks at higher energy.



Zhang & Böttcher (2013)

Leptonic vs. Hadronic Emission

These data show how an instrument like AMEGO will be able to determine the jet composition.



Summary

Prospects for the future of MeV polarimetry are very exciting.

Several exciting areas of research:

- gamma-ray bursts
- solar flares
- pulsars
- X-ray binaries
- AGN (Blazars)

New instrumentation:

- next-generation MeV instruments (e.g., COSI-X, AMEGO, e-ASTROGAM)
- dedicated GRB polarimeter instruments (e.g., POLAR, GRAPE)
- imaging polarimeters for solar flares (e.g., GRIPS)